Integrating multi-functional space and long-span structure in the early design stage of indoor sports arenas by using parametric modelling and multi-objective optimization

Pan, Frank; Turrin, Michela; Louter, Christian; Sariyildiz, Sevil; Sun, Yimin

Important note
To cite this publication, please use the final published version (if applicable).
Please check the document version above.

Integrating multi-functional space and long-span structure in the early design stage of indoor sports arenas by using parametric modelling and multi-objective optimization

Wang Pan[a,b], Michela Turrin[b], Christian Louter[c], Sevil Sariyildiz[b], Yimin Sun[a,*]

[a] School of Architecture, State Key Laboratory of Subtropical Building Science, South China University of Technology, Guangzhou, China
[b] Chair of Design Informatics, Faculty of Architecture and the Built Environment, Delft University of Technology, Delft, the Netherlands
[c] Chair of Structure Design, Faculty of Architecture and the Built Environment, Delft University of Technology, Delft, the Netherlands

ARTICLE INFO

ABSTRACT

Indoor multi-functional sports arenas are a complex building type. Integration of the (multi-) functional space and of the large-span structure of the roof mainly determines the overall geometry of the building, and is one of the most challenging phases of the design. Several interdisciplinary numeric assessments and numerous solutions with diverse geometries (rather than just several specific types) should be considered to make informed design decisions.

To support the design exploration in the early design stage for multi-functional arenas, this paper proposes a design process that is composed of a flexible parametric model, a framework of interdisciplinary assessment criteria, and multi-objective optimization (MOO) with post-process tools. The parametric model is defined based on the basic spatial composition of arenas and is flexible to provide a broader design space, including diverse solutions with three frequently-used structural types. The framework of assessment criteria includes indicators of viewing quality for spectators, acoustics, and structures, which can evaluate the design in different aspects. Based on certain assessment criteria, the MOO can be used to search for good designs in the broader space, and the post-process tools facilitate the designer to analyse the results. Two typical arenas (the Barclay Centre and the O2 Arena) are selected as real case studies to demonstrate the proposed process and assess the capacity. Results of the case studies validate the efficacy of the process and the necessity of the broader design space to include diverse solutions with multiple structural types.

1. Introduction

In design practice, the importance of integrating functional space and structure is emphasized by architects and engineers. In fact, these two aspects are usually interrelated and their integration mainly defines the overall geometry of the building. This integration is especially crucial for the conceptual design of indoor sports arenas (Fig. 1A). For an indoor arena, the functional space is usually multi-functional (that needs to cater to different activities) and requires a long-span roof structure. The outline of the multi-functional space defines the boundary and the span of the long-span structure, which impact the structural performance (Fig. 1B). At the same time, the geometry of the structure impacts not only the structural performance but also the functions of the multi-functional space (Fig. 1C and D).

To achieve this integration during the early design stage, several architectural and structural aspects and their interrelations should be

considered to generate good design solutions. With the rapid development of digital and information technologies, computational design is widely used to support architectural conceptual design. In computational design, computational tools, methods, and techniques are used to enable designers to encode the design requirements and rules into algorithms that generate alternative designs for buildings [1]. Computational design is also considered as a study of how programmable computers can be integrated into the process of design by developing computer algorithms [2].

Nowadays, several computational processes are commonly used during the design process, including design optimization. Among several possible approaches, a framework named performative computational architecture is proposed [1]. This framework consists of form generation based on parametric modelling, performance evaluation based on numeric assessments and simulations, and multi-objective optimization (MOO). These three components are iterated in order to
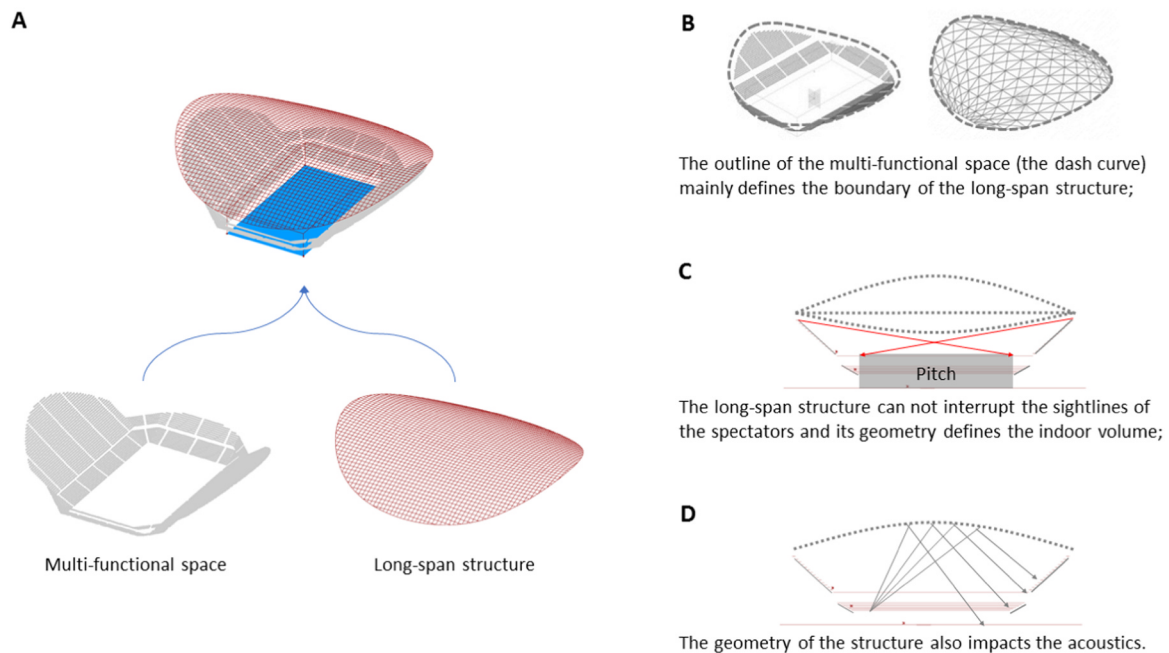

Fig. 1. The composition of a sports arena.

generate and assess a large number of design alternatives. Similar approaches are used by several designers and researchers to support integrated design [3,4]. In such a process, parametric modelling allows the association of elements of the building and generate numerous design alternatives while guaranteeing predefined geometric relations. Different aspects (e.g. structure, HVAC, energy, acoustics, daylighting) of the design alternatives can be evaluated by simulations. Among the design alternatives included in the optimization process, the ones which perform better can be found according to specific assessment criteria related to the design requirements.

In this general approach, this process shows remarkable potential to support the design of sports arenas. However, the workflow should be customized based on the specificities of sports arenas. In fact, though various aspects have been combined into architectural conceptual designs based on design optimization, little attention has been paid to the integration of the multi-functional space and long-span structure of sports arenas.

Hence, this paper proposes a novel design process based on parametric modelling, numeric assessment criteria and multi-objective optimization. It aims at integrating the multi-functional space and long-span roof structure for the early design stage of sports arenas, with emphasis on the diversity of design alternatives and the variety of the numeric assessments.

The proposed process focuses on the early design stage of sports arenas. In this stage, a design exploration of geometries based on both architectural and engineering aspects is crucial for selecting overall geometries of the building [4]. Designers can select the aspects of interest to formulate numeric assessment criteria and use optimization to guide the exploration (Fig. 2A). Integrating these aspects in design exploration aims at finding suitable design solutions for the following design stage. It does not mean the specific designs for these aspects can be replaced. Indeed, when some solutions have been selected based on the design exploration, all the aspects related to the overall design requirements should be deeply considered in the following design stage(s) to define a final design concept (Fig. 2B).

Specifically, for a design exploration, the diversity of design alternatives is crucial. Traditional parametric modelling approaches usually focus on a specific type of solution in each design. As a result, although there can be numerous solutions in the design space, they may be

similar in geometry (the upper path in Fig. 2A). However, in practice, designers usually prefer to study diverse design geometries [2]. Moreover, different types of geometries may perform differently in various aspects. Therefore, a broader design space including diverse types of geometries, rather than a design space with one or two types of geometries, is crucial for design explorations (the bottom path in Fig. 2A). Within this context, Harding proposed a meta-parametric design tool ('Embryo') allowing designers to explore geometries with different topologies [2]. For indoor sports arenas, although the topology of the multi-functional spaces is fixed (a pitch surrounded by a seating bowl with a roof cap), the typology can be varied. The seating bowl can be round, rectangle, polygon, oval, or irregular form, and the geometry of the roof can be a surface of plane, zero Gaussian (e.g. vault), positive Gaussian (e.g. dome), negative Gaussian (e.g. saddle) or free-form. Therefore, with a fixed topology, it is necessary to provide a broader design space, including various types of possible geometries for the design exploration of sports arenas, which is emphasized by the proposed design process.

The variety of numeric assessments is also crucial for the optimization-based exploration. In design practice, there are many numeric indicators can be used to assess the multi-functionality and structure of arenas. The assessment criteria related to different indicators can lead to different results for the optimization. To adapt to various design conditions in practice, it is necessary to provide a framework of assessments including various indicators, rather than a fixed set of criteria.

2. Background and related works

2.1. Integration of the multifunctional space and long-span structure in sports arena design

The multi-functional space, which is the core space of sports arenas, usually serves for various sports competitions, stage performances (e.g. concerts, dramas), exhibitions, and daily sports for the public, etc. Such space, which is usually called the 'bowl' by designers, is composed of a pitch and seating tiers (stands), and the long-span roof can be seen as its cap. (Fig. 1A)

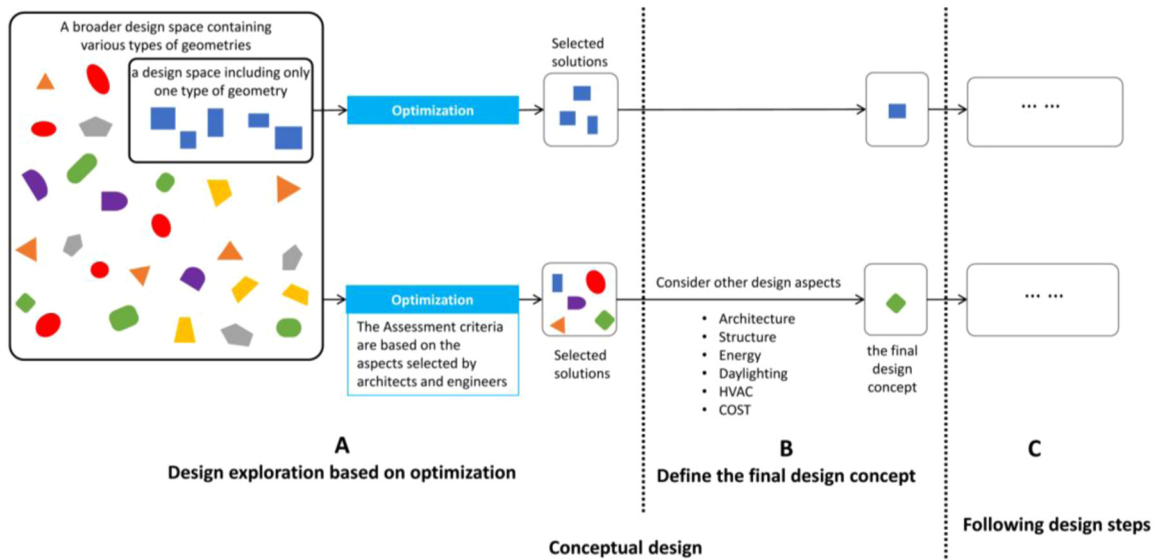The pitch is the bottom of the bowl and its dimensions determine

Fig. 2. The diagram of the overall design process (the various colourful shapes in the boxes represent different types of design).

Table 1
Pitch dimensions for different activities [10,11].

Activities		Area of court/stage/exhibition booth Length × width × height (m)	Overall Area Length × width × height (m)
Sport event	Ice hockey	61 × 26 × 6	65 × 36 × 6
	Gymnastics Artistic	60 × 34 × 10	68 × 42 × 10
	Handball	40 × 20 × 12	50 × 28 × 12
	Basketball	28 × 15 × 9	32.1 × 21.1 × 9
	Football (five-a-side)	50 × 35 × 7.5	56 × 41 × 7.5
	Volleyball	18 × 9 × 12.5	31 × 22 × 12.5
	Tennis (indoor)	36.57 × 18.29 × 12	49.37 × 25.61 × 12
	Gymnastics Rhythmic	13 × 13 × 12	21 × 21 × 12
	Trampoline	28 × 12 × 12	36 × 20 × 12
	Wrestling	8 × 8 × 3.5	14 × 14 × 3.5
	Judo	8 × 8 × 3.5	14 × 14 × 3.5
	Taekwondo	8 × 8 × 3.5	14 × 14 × 3.5
	Badminton	13.4 × 6.1 × 12	17.4 × 10.1 × 12
	Table Tennis	14 × 7 × 5	14 × 8 × 5
	Short track speed skating	61 × 26 × 6	65 × 36 × 6
	Figure skating	61 × 26 × 6	65 × 36 × 6
Stage performance	concert	Defined by developers	
	drama		
	Assembly/speech		
Exhibition		Booth:3 × 3 × 3	Calculated based on the number and arrangement of the
		width of aisle: 3	booth
Daily sports for the public	4 (badminton) courts[a]	13.4 × 6.1 × 12	33 × 18 × 12
	6 (badminton) courts[a]		33 × 27 × 12
	8 (badminton) courts[a]		37 × 33 × 12
	9 (badminton) courts[a]		51 × 27 × 12
	12 (badminton) courts[a]		54 × 33 × 12

[a] According to 'Sports Halls: Sizes and Layouts' provided by SportsEngland [10], the pitch of daily sports for the public is defined based on a module of a badminton court.

which activities can be accommodated according to the spatial requirements (Table 1). It also determines the inner outline of the seating tiers which are set around the pitch. The arrangement and dimensions of seating tiers are designed according to design codes. This paper focuses on the European code (EN 13200) for spectator facilities [5], which regulates a series of sizes for seating tiers (e.g. the sizes of the seats and rows, the number of seats between gangways, the width of a gangway, and the riser of each row).

Therefore, based on the design codes, two design variables mainly determine the overall shape of the 'bowl': the inner outline determined by the pitch (Fig. 3A and B) and the outer outline (Fig. 3C). It means

that for most arena designs, one of the most import design tasks of the 'bowl' is defining the pitch dimensions and the outline of the multi-functional space. Furthermore, the geometry of the 'bowl' determines the accommodation of different activities, spectators' viewing quality for different events, and acoustics. These aspects are related to the basic functions of the multi-functional space of a sports arena.

Some previous work has used parametric modelling to generate multi-functional spaces. Hudson formulated a reusable parametric model for the grandstand of an outdoor stadium [6]. Similarly, Sun et al. formulated a flexible model for the one-side grandstand of stadiums by using shape grammar in parametric modelling software [7].
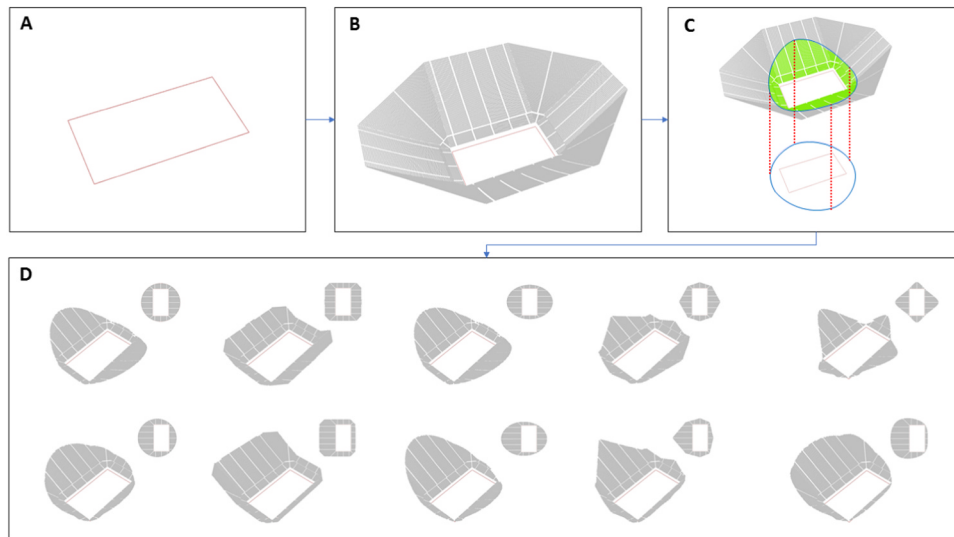
Fig. 3. The seating bowl defined by the outlines of the pitch and the multi-functional space (A: the outline of the pitch; B: the foundation of the seating bowl generated based on the pitch and the regulations in design codes [5] ; C: seating bowl defined by the outline of the multi-functional space; D: some examples of the seating bowls generated by different outlines of the multi-functional space).

This model allows designers to define the geometry of the grandstand by changing the outline. Additionally, the engineering firm Arup proposed StaG (Stadium Generator) which is a parametric model of the seating bowl for stadiums [8,9]. However, these models did not consider roof structures.

The long-span roof structure can be considered as the 'cap' of the 'bowl'. The outline of the 'bowl' mainly determines the boundary of the long-span structure, which defines its span and supports and influences its geometry. The structural geometry influences not only the structural performance but also the indoor functions. For one thing, the roof structure cannot invade the clear space of the pitch or interrupt the sightlines of spectators. For another, the geometry of the roof also determines the indoor volume, which is crucial for acoustics.

Some previous work has combined the multi-functional space and structure. Miller formulated a parametric model to generate design alternatives of the seating bowl and combined them with a specific roof structure for stadiums [12]. Hudson et al. proposed a parametric design process for Aviva Stadium, which integrates the envelope geometry, structure, and cladding in a parametric model, according to an existing design concept [13,14]. Holzer proposed a similar model for stadium designs [15]. Although these models combine the seating bowl and structure, they are fixed for specific designs rather than flexible models which contain diverse types of design alternatives.

Some previous work has focused on performance. For the assessment of the multi-functional space, the viewing quality of spectators and the room acoustics (for stage-performance) are emphasized by researchers. To assess the views of spectators, Xiong et al. used viewing distance, sightline obstruction ratio, horizontal/planar viewing angle, vertical viewing angle, torsion angle, and the field of vision as the indicators [16]. Hudson et al. proposed 'A-values' to indicate spectator's vision field [17]. For the room acoustics, reverberation time (RT_{60}), initial time delay gap (ITDG), brilliance, warmth, etc. are important indicators for the assessment [18]. For the assessment of long-span structures, structural self-weight (mass), strain energy, structural mass/self-weight, and embodied energy are used by researchers. Von Buelow used structural self-weight (mass) as one of the objectives to optimize a water tower, a truss road bridge, and a geodesic dome, respectively [19]. Cui et al. considered architectural factors during the structural optimizations of discrete frame structures for a dome roof and used strain energy to evaluate structures [20]. Brown et al. used embodied energy to evaluate long-span structures [21]. The value of embodied energy is obtained by multiplying the structural mass/self-weight by a coefficient provided by Hammond [22]. Nevertheless, there is a lack of comprehensive assessment criteria which can be used to simultaneously evaluate the aspects of multi-functional space and long-span structure.

2.2. Design optimization

As a design process which is widely used to support integrated and performance-driven designs, design optimization can be composed of several methods. The one considered in this paper is composed of parametric modelling, building performance simulations/analyses, and a searching algorithm.

Parametric modelling is defined as a process of formulating a geometrical representation of a design with parametrized components and attributes [23]. In the process, designers develop a parametric model which is based on relationships between objects controlled by parameters [6,2]. By changing the values of the parameters, the model can be changed to generate numerous design alternatives. Such design alternatives constitute a design space.

Performance simulation is used to imitate, to some extent, real-world conditions for design alternatives and to obtain the values of related indicators. For example, finite element analysis (FEA) is used to simulate different loads for structures, and calculate the indicators, such as mass/self-weight, strain energy, stress, strain, displacement, etc. These indicators are then formulated into design objectives and constraints for optimization, according to the assessment criteria formulated by designers.

To find well-performing solutions in a design space containing numerous design alternatives, optimization with a certain searching algorithm can be used [24]. During optimization, with the design constraints $g(X)$ and $h(X)$, the value of the objective function $f(X)$ is minimized or maximized using a search algorithm to systematically select proper sets of variables X, which can be expressed by mathematic formulae [25]:

$$Min. \quad f(X) \tag{1}$$

$$\text{subject to} \begin{cases} g(X) \leq 0 \\ h(X) = 0 \end{cases}$$

where $X = [x_1, x_2 \dots x_i \dots x_n]$ (n is the number of the variables of each solution)

In real-world building design problems, there are usually several conflicting objectives, and multi-objective optimization (MOO) is necessary [26,27]. To solve the problem of the conflict among different objectives, the concept of Pareto optimality is an option, which provides a set of Pareto solutions that are not dominated by each other [24].

For most complex engineering projects, the relationships between variables and design objectives are complex and implicit. In other words, there is a complex relationship between the inputs and outputs, which is a black box for the optimizer. As a result, stochastic optimization is used, in which a search algorithm is used to find satisfactory alternatives by iterations. Heuristic algorithms (such as genetic algorithm, simulated annealing algorithm, particle swarm, Tabu search, etc.) are widely used for the stochastic optimization in building design. Among them, the genetic algorithm is the most frequently-used, according to the statistics from Evins [28] and Nguyen et al. [24].

These kinds of design optimizations have been applied to the architectural conceptual design of complex buildings in many research works. Among the many possible examples, Keough and Benjamin optimized a pavilion according to structural performance and the consumption of material [29]. Turrin et al. used design optimization for a large roof based on the consideration of climate and daylighting comfort [30]. Shi et al. optimized a complex roof surface and a box building with the consideration of solar radiation and energy consumption [31]. Lin et al. used design optimization for complex buildings to deal with spatial programme compliance, energy consumption and cost [32]. Mueller et al. used design optimization for the lateral and gravity structural system of an airport terminal according to structural performance and design preference [33]. Brown et al. optimized the geometry of roof structure and envelope for long-span buildings to reduce the embodied energy and operation energy, and to study their inter-relationships [21].

Specifically, for the design optimization applied for sports building, Holzer et al. studied how the process including parametric modelling, structural analysis, and optimization assists architects and engineers to perform a conceptual design of a stadium roof [15]. Yang et al. proposed a series of approaches for the design explorations and optimizations of sports halls, which focus on the aspects of daylighting, energy, and structure [34–36]. Turrin et al. proposed several methods of design exploration and optimization for sports buildings, which focus on structure, daylighting, ventilation, and energy [37]. Although these works have provided various methods for the design optimization of sports arenas to integrate different aspects, little attention is paid to integrations of the multi-functional space and structure for indoor arenas.

2.3. Diverse typology of design alternatives

For conceptual design, the diversity of design alternatives is crucial. Harding observed that designers prefer to formulate various, quite different design concepts during the early phase of conceptual design [2]. Brown et al. pointed out that there are various architectural forms and responding building shapes and structural systems that could be optimized for performance, and it is important to develop methodologies to produce design examples that are applicable to a wide range of building geometries [21].

To ensure the diversity of designs in design optimization, two aspects are crucial: the diversity of the design alternatives (generated by parametric model) in design space [2] and the diversity of the solutions that are selected (from the alternatives) by optimization [33,38,39].

The diversity of the design alternatives in design space mainly depends on the flexibility of the parametric model [2]. Shea et al. stated that designers should model a conceptual structure leading to variation [40]. Harding proposed a meta-parametric modelling method based on genetic programming [2]. This method allows dynamic generations of parametric definitions, which leads to a flexibility in the topology and typology of the parametric model. Brown et al. considered three different design concepts in multi-objective optimization [21]. In consequence, the results are diverse in geometry, and the relationships between geometry and performance were deeply studied.

For sports arenas, the building topology is fixed (a bowl shape with a cap). To ensure the diversity of the alternatives, the parametric model should be flexible to generate bowls and caps with diverse shapes. Furthermore, since different types of structures are usually matched to different spans and geometries [41,42], it is necessary to consider multiple structural types to ensure a good match with the diverse geometries.

Based on the diversity of design alternatives, the diversity of the final solutions selected by optimization can be enhanced by some operations of the searching algorithm in optimization. Von Buelow proposed a genetic algorithm-based platform for performative exploration, called 'ParaGen', in which designers can interactively control the selection and breeding steps in each generation of the genetic algorithm, according to criteria that are not included in the fitness function (e.g. aesthetics and other soft requirements) [19,38]. One of the aims of this method is to provide multiple solutions during the exploration. Similarly, Mueller et al. provided an interactive optimization for designers to explore a design space of structures by addressing qualitative design goals and constraints for human designers [33]. Based on this interactive evolutionary algorithm, designers can explore diverse solutions by increasing the mutation rate during iterations. Nonetheless, these operations may lead to reductions in performance [33]. Harding proposed a design method "Biomorpher", which combines parametric modelling with an interactive clustering-orientated genetic algorithm, to allow designers to select designs according to motivations besides performance criteria in each generation of the evolution [39].

2.4. Limitations and further requirements

Based on the analyses of the precedents, the state of the art shows some limitations that hinder the integration of multi-functional space and structure in the design of sports arenas. First, there is a lack of design optimization process specifically customized for the integration of the multi-functional space and long-span structure in sports arena designs. In addition, there is also a lack of comprehensive assessment criteria on the aspects of multi-functional space and long-span structure for sports arenas. Furthermore, in most of the design optimization processes for architectural conceptual design, each parametric model includes parametric variations of only one specific geometric typology, which limits the diversity of design alternatives in the design space and hinders the exploration of various possibilities in early design stages.

To overcome these limitations, a specific design process is proposed for sports arena designs. Such a process facilitates designers to integrate the multi-functional space and long-span structure, to provide diverse types of design alternatives, and to select the solutions according to the requirements of multi-functionality (in this paper it includes the aspects of accommodation of different activities, spectators' view, and acoustics) and structure.

3. Proposed design process

The workflow of the proposed process is illustrated in Fig. 4. First, a flexible and versatile parametric model for sports arenas is proposed, based on Rhino [43] and Grasshopper [44] (Fig. 4A). This model integrates the multi-functional space and long span structure and includes diverse types of geometries for sports arenas. Besides, considering that different structural types prefer certain geometries [41], three types of frequently-used long-span structures (grid-shell, space-frame, and truss-beam) are applied in the model, to ensure the diversity of the roof geometries. The detail of the model is elaborated in the sub-Section 3.1.

Then, a framework of assessment criteria is proposed to evaluate solutions based on specific performance (Fig. 4C). This framework combines indicators of the basic aspects of multi-functionality (accommodation of activities, views of spectators, acoustics) and structure. The related values of the indicators for each design alternative are obtained by simulation tools (Fig. 4B). The details of the assessment criteria and simulations are elaborated in the sub-Section 3.2. Multi-objective optimization (MOO), which is performed by the optimization
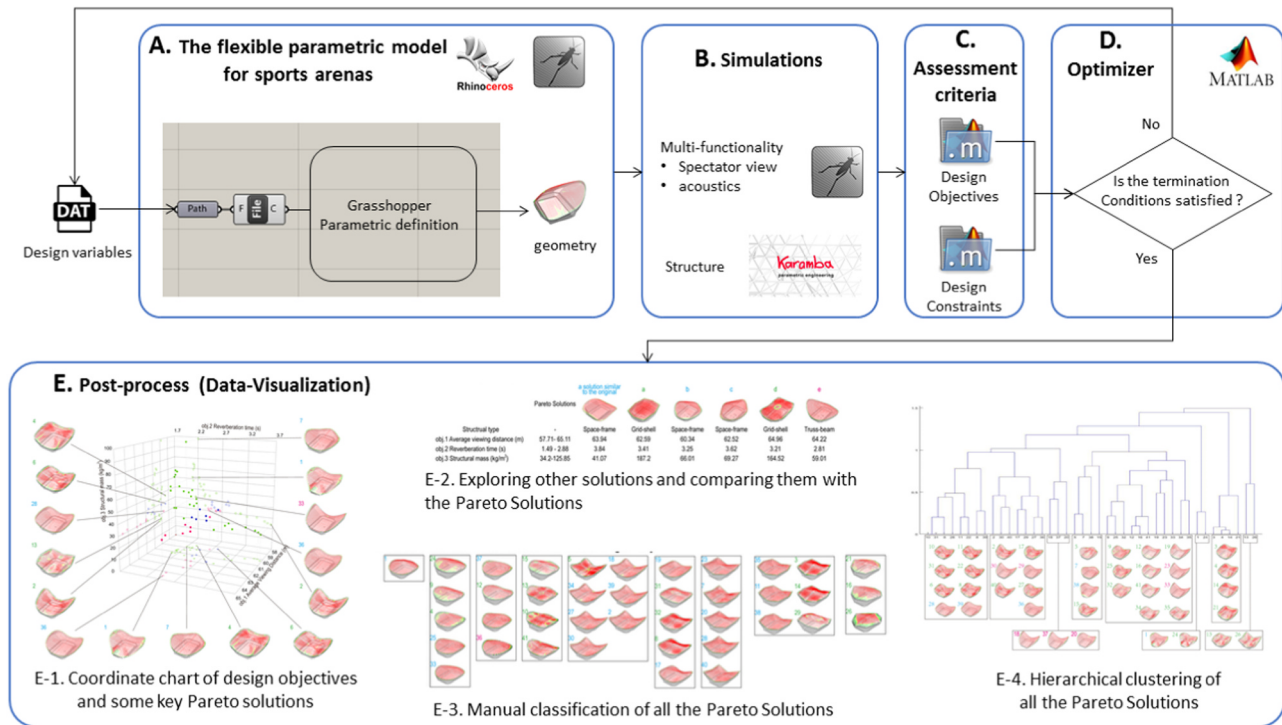
Fig. 4. The workflow of the proposed design process.

toolbox of MATLAB [45] with NSGA-II [46] as the search algorithm (since this ongoing project will use other toolboxes in MATLAB in the following steps), is used to search satisfactory solutions within design space according to the criteria (Fig. 4D). Finally, a set of post-process approaches are used to visualize the results (Fig. 4E). A 3D coordinate chart of the objectives of all the Pareto solutions and the geometries of some key Pareto solutions are provided to visualize the optimization results (Fig. 4E-1). Based on the history of the iterations stored during the optimization, the solutions weeded out during the optimization can be also selected to demonstrate and compare with the Pareto solutions (Fig. 4E-2). Furthermore, designers can classify the Pareto solutions according to their geometries (Fig. 4E-3) to explore and select final solutions according to some soft requirements (e.g. aesthetics). If the number of the Pareto solutions is too large, a hierarchical cluster analysis can be used to automatically group them according to their geometric typology (Fig. 4E-4) The detail of the optimization and the hierarchical clustering are elaborated in the sub-Section 3.3.

3.1. A versatile parametric model for sport arenas

According to the previous analysis of the interrelationships between the multi-functional space and long-span roof structure of arenas, the proposed parametric model is defined in four steps. Table 2 illustrates the process and lists related parameters. It is worth noting that even though this model includes most formal types of sports arenas, some special types (e.g. arena with discrete roof which is composed of several surfaces) are not yet included. For the long-span structure, this model only focuses on three frequently-used lattice steel structures (grid-shell, space-frame, and truss-beam) with a quadrilateral topological pattern.

Step 1 deals with the pitch and the foundation of the seating bowl (Table 2, step 1). The dimension of the pitch can be determined according to the activities which are planned to be held in the arena (Table 1). In this step, designers should select a principal activity to define the focal point for spectators' sightlines and generate the seating tiers. Sections of tiers and the rows for each section should also be defined. In this paper, a method, which uses one or several specific 'values of V' to calculate the riser of each row (C), is used to generate

the foundation of the seating bowl. Fig. 5 illustrates the calculation, and the riser of each row (C) can be calculated based on the formula provided by the design code EN 13200 [5]:
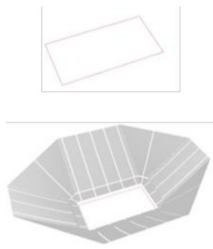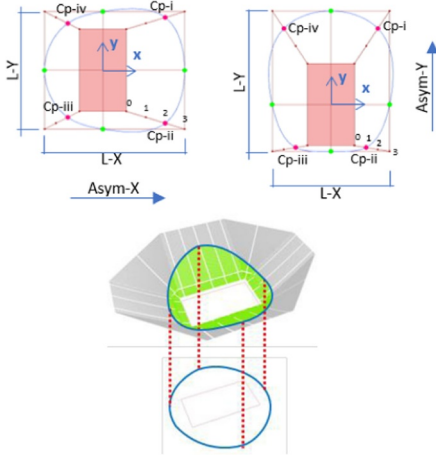
$$C = V + \frac{a \times B}{D} \# \tag{2}$$
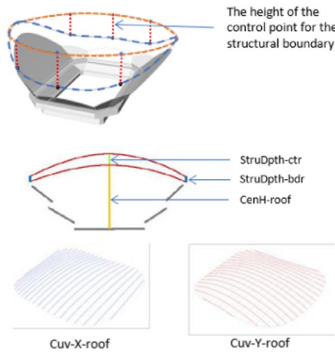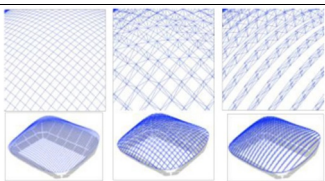
where C is the riser of the row, V is the vertical distance from eyes of a spectator to the top of the head (see V in Step 1, Table 2), a is the difference between the height of eyes and the height of focal point P (the nearest point of focus along the line of sight), B is the distance from one spectator to the spectator behind (which equals the '*Depth-SR*' in Step 1, Table 2), D is the horizontal distance between the spectator's eyes situated and the focal point P.

In step 2, a variable building outline is formulated to trim the foundation of the seating bowl and generate the final bowl (Table 2, step 2). The outline is defined by eight control points and the curve type (polyline or curve). The control points are defined by the lengths along the X and Y axes, the asymmetric ratios in x- and y-axis, and the corner positions. Thus, diverse multi-functional spaces can be generated (Fig. 3). The number of fixed seats for the seating bowl should be examined in this step. The height of the last row of seating bowl is related to the lengths along the axes and the shape of the foundation bowl, which should be constrained according to design requirements in practice. In fact, the height can be varied in a large range for different sizes of the buildings. For the Philippine Arena (50,000 fixed seats), which is the largest indoor arena in the world, the height for the last row is around 60 m [47].

Based on the seating bowl, step 3 formulates the roof by quadrilateral grids (Table 2, step 3). First, the structural boundary is generated by eight control points related to those in step 2. The initial positions of the points are on the seating bowl boundary (the blue dash curve in the first chart of step 3 in Table 2), then the points (except the highest ones) are allowed to move to any position between the original position and its highest position (with the same height as the highest control point). This method allows the structural boundary to vary between the seating bowl outline and the flat structural boundary (the orange dash curve in step3 of Table 2). Sequentially, based on the

Table 2
Process and parameters of the proposed parametric model.

Step	Parameter	Description
Step 1	P-size	Dimensions of the pitch, decided by designers according to design requirements
	Seat-Num	Amount of the fixed seats, decided according to design requirements
	SE_{PRI}	The court size of the principal activity for sports event
	V*	C-value: the vertical difference from eyes of a spectator to the top of the head: 120mm (Recommended)
	Depth-SR*	Depth of the seating-row: ≥0.8m
	Width-S*	Width of a seat: ≥ 0.5m
	Nur-SR*	Number of the seats between radical or parallel passageways: ≤ 28
	Width-PW*	Width of a passageway: ≥ 1.2m
	Seat-Sec	Number of the sections of the seating tiers
	Row-Sec	Number of rows for each section
Step 2	L-X	Length of the building along the X axis
	Asy-X	Asymmetry in X-axis (for the performance of side-stage) – Range: 0 to 1 – 0: symmetric in X-axis – 1: totally asymmetric in X-axis
	L-Y	Length of the building along the Y-axis
	Asy-Y	Asymmetry in Y-axis (for the performance of end-stage) – Range: 0 to 1; – 0: symmetric in Y-axis; – 1: totally asymmetric in Y-axis.
	Cp-i Cp-ii Cp-iii Cp-iv	Corner positions in 1st, 2nd, 3rd, and 4th quadrant: – Range: 0, 1, 2, 3; – 0: overlap with the corner of the pitch; – 3: overlap with the corner of the outer rectangle.
	Cuv-BO	Curve type of the building outline: – 1: polyline (one-degree curve); – 3: curve (three-degree curve).
Step 3	H-CPi-bdr	The height of the ith control point of the structural boundary 0 to 10 when the variable equals to 0, the control point is on the original boundary parallel to the seating bowl outline (the blue one; when it equals to 10, the control point is as height as the highest control point and is on the orange curve.
	CenH-roof	headroom of the centre of the pitch: ≥ 18m
	GridSize-roof	Size of the grid, can be varied according to structural type
	Cuv-X-roof	Curve type of the grid in X and Y axes: – 1: polyline;
	Cuv-Y-roof	– 3: curve.
	StruDpth-ctr	Structural depth in the centre (for space frame and truss beam)
	StruDpth-bdr	Structural depth on the boundary (for space frame and truss beam)
Step 4	StruType	Structural type: – 0: Grid Shell (GS); – 1: space frame (SF); – 2: truss-beam along x-axis (TB in X); – 3: truss-beam along y-axis (TB in Y).
	Dia-Sec	Sectional diagram and Sectional thickness (selected by optimization within the ranges defined by users; Unit: cm).
	Th-Sec	
	Material	Steel (S235, S275, S335)

* regulated by design code EN 13200 [5].

structural boundary, a single-layer grid is formulated according to several parameters: the headroom of the central point in the pitch, the curve degrees in x and y dir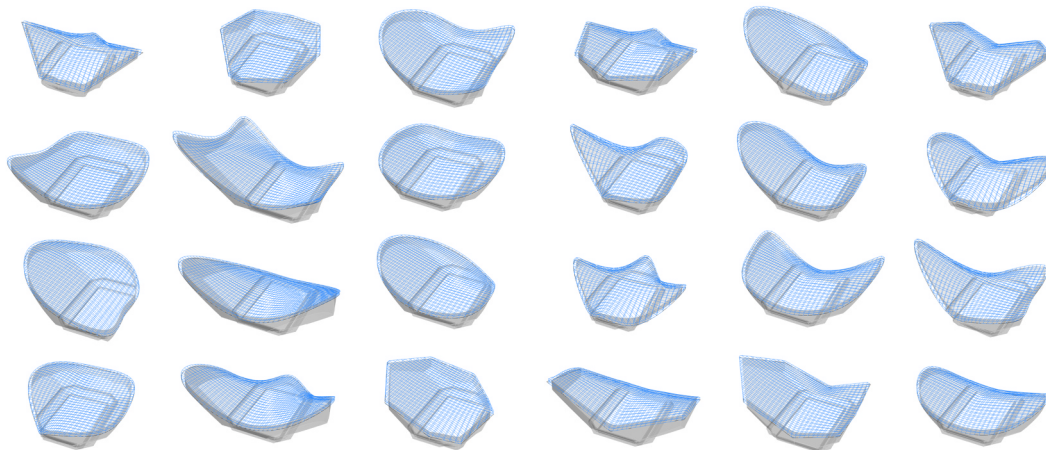ections, and the spacing of the grid (the spacing can be varied according to the structural type). Based on this grid, an upper layer grid is formulated by adding structural depths in the centre and on the boundary, respectively. The two depths are

Fig. 5. The diagram of the riser calculation [5].

independent, therefore, the relationships between them can be varied (linearly or non-linearly). Additionally, the grid can be curves or polylines in x and y directions, respectively, which are controlled by two parameters (Cuv-X-roof and Cuv-Y-roof). Various roof geometries can be generated based on this step.

Step 4 generates three different structural types, based on the grids (Table 2, step 4 and Fig. 6A and B). This paper does not deal with the structural topology optimizations but uses specific topological pattern. For grid-shell (GS), a quadrilateral pattern is used, the bottom-layer grid (Fig. 6A) can be directly used as the axes of the elements (bars). For space frame (SF) and truss beam (TB), a two-layers of grids are necessary. Based on the original grid (the red one in Fig. 6A and B), an upper grid (the blue one in Fig. 6B) is generated according to two parameters, SturDpth-ctr (structural depth in the centre of the roof) and StruDpth-bdr (structural depth on the boundary of the roof). For space frame, the upper grid and the bottom (original) grid are directly used as the axes of

the upper and bottom chords, additional vertical and diagonal webs are added between them (Fig. 6C). For truss-beam (TB), both the x- and y-axis can be the span direction of the beams, which are considered as two sub types for TB. The cross-section of each truss beam is an inverted triangle (Fig. 6D), which is composed of two upper chords (generated by offsetting the upper grid lines) and one bottom chord (directly generated by the bottom grid lines). Additional webs are set between the chords. For all the structural types, steel (S235, S275, or S335) is used as the material, and hollow circles are selected as the sectional shape for the elements. Designers should assign the ranges of the diameter and thickness of the section.

Based on the proposed parametric model, a broader design space with diverse geometries for sports arenas can be generated, which includes not only some conventional geometries (examples are proposed in Fig. 7A) but also some special ones (examples are proposed in Fig. 7B). It can also be used to mimic the geometries of real arenas with

Fig. 6. The generation of the roof structure.

A: Some regular geometries in the design space

B: Some irregular geometries in the design space

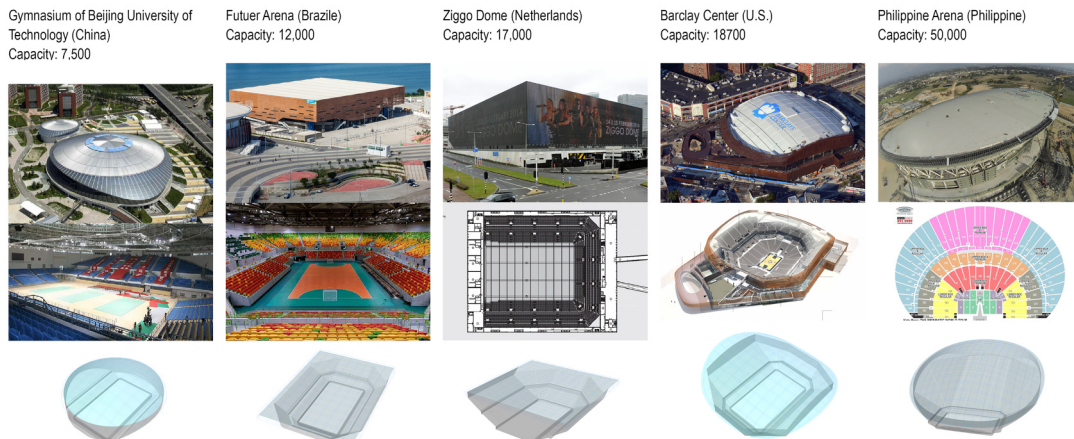**C: Examples of some real arenas in different sizes and geometries**

Gymnasium of Beijing University of Technology (China) Capacity: 7,500

Futuer Arena (Brazile) Capacity: 12,000

Ziggo Dome (Netherlands) Capacity: 17,000

Barclay Center (U.S.) Capacity: 18700

Philippine Arena (Philippine) Capacity: 50,000

Fig. 7. Some examples within the design space generated by the proposed parametric models (the sources of the pictures in part C [48–57]).

different shapes and sizes (examples are proposed in Fig. 7C). The feasibility of the geometries can be guaranteed by setting the ranges of variables (e.g. the size of the building, the height of the roof) and the constraints of some indicators (e.g. the number of fixed seats, the maximum viewing distance of spectators, the maximum deflection viewing angle of spectators).

3.2. Assessment criteria and simulations

As mentioned in the sub-Section 2.4, the accommodation of activities, spectator's view and acoustics are considered as the basic functions of the multi-functional space of a sports arena in this paper. The assessment criteria are formulated based on these aspects and the long-span structure.

The accommodation of various activities, in design practice, is usually set by developers and designers before conceptual design according to the dimensions of these activities (Table 1).

3.2.1. Viewing quality of spectators

This paper focused on five indicators for the viewing quality of spectators:

- VD_{avr-p}: the average viewing distance for the principal activity of the arena;
- VD_{max-e}: the maximum viewing distance of different activities;
- OR: the sightline obstructed ratio;
- RM_{HVA}: the ratio of the seats used for stage performance;
- RS_{P-HVA}: the ratio of the seats with premium horizontal viewing angle for stage performance.

The viewing distance (VD) of a spectator for a specific activity is the distance between the spectator's eyes to the farthest point of the activity area (left, Fig. 8). The average and the maximum values (VD_{avr} and VD_{max}) of VD can be minimized (as design objectives) or limited into certain ranges (as design constraints), to enhance the viewing quality or ensure an acceptable view for each spectator. The European code for spectator facility (EN 13200) regulates the thresholds of viewing distances for different activities [5]. It is worth noting that, the viewing distance varies according to different activities, since they have different focal points. In practice, designers and developers usually select important and frequently-held activities as the principal activities and the others as secondary activities [10]. Then, the indicators related to the principal activities can be minimized or maximized to enhance the related viewing quality, and the indicators of the secondary activities are set as constraints to ensure acceptable viewing quality.

The sightline obstruction ratio (OR) of a spectator is defined as the ratio between the number of obstructed sampling points (the sampling points on the pitch but obstructed by other spectators) and the number of total sampling points on the pitch (Fig. 8, right) [16]. In practice, the obstruction is usually avoided by setting a proper C-value to calculate the riser for each row (see Fig. 5 and formula 1) and to generate the seating bowl. However, the focal point for the riser calculation is related to the selected principal activity, if the court size of the principal activity is much smaller than the pitch, the area inside the pitch but outside the principle court may not be seen by the spectators. In this case, OR can be used to assess the visibility of the area outside the principle court but inside the pitch [16]. For other cases, a proper

selection of the focal point and C-values can guarantee the activities are visible for spectators.

It is worth noting that all the seats around the pitch can be used for sports events, while only a subset of them can be used for stage performance. The subset is defined by a horizontal viewing angle (HVA) and its reference points (RP_{HVA}) (Fig. 9, left), is used to defined the accepted seats for stage performance. These parameters can be set by designers according to specific requirements of performance. In design practice, it usually requires as many seats as possible to be used for different activities. To assess the fulfillment of this requirement, this paper proposes the ratio of multi-functional seats (RM_{HVA}) as the indicator. RM equals the number of the accepted fixed seats for stage performance divided by the number of all the fixed seats. It can be also maximized as a design objective or limited in a specific range as a constraint. Furthermore, based on the accepted horizontal viewing angle mentioned above, a smaller angle, premium horizontal viewing angle (P-HVA) is proposed (Fig. 9, right). The PHVA is used to define the premium seats for the stage, which have better view for stage performance. The ratio (RS_{P-HVA}) between the numbers of these premium seats and the total seats can be used as another indicator to assess the seating bowl for stage-performance.

3.2.2. Acoustics

For acoustics, among the mentioned indicators, this paper focuses on reverberation time (RT_{60}), since it is related to the configuration of the indoor space which is mainly defined during conceptual design. The requirements on other indicators can be satisfied in professional acoustic design. RT_{60}, which is defined as the time for a sound to drop 60 dB below its original sound level, can be calculated by the Sabine Formula [58]:

$$RT_{60} = \frac{0.161 \cdot VL}{A + 4m \cdot VL} \qquad (3)$$

$$A = \sum S_j a_j \qquad (4)$$

VL is the effective volume of the reverberation space; A is the total absorption within the room; m is the average absorption coefficient of the air; S_j is the area of the jth inner surface of the room; a_j is the absorption coefficient of the jth inner surface (see Table 3). According to the Sabine Formula, RT_{60} can be obtained by measuring the volume and surface area in the parametric model. According to the activities emphasized in the design, the RT_{60} should be calculated based on all the related octave band frequencies, respectively, and the average value is used to assess the design. For example, for sports events, the middle frequencies around 1k Hz are emphasized, while for concerts, all the frequencies from 125 Hz to 4 kHz should be considered.

Different activities require different reverberation times (Fig. 10), and it is difficult to meet the different requirements at the same time [58]. For example, the crowd sound made by spectators is important for the atmosphere of sports events, and a larger value of RT_{60} is preferred.
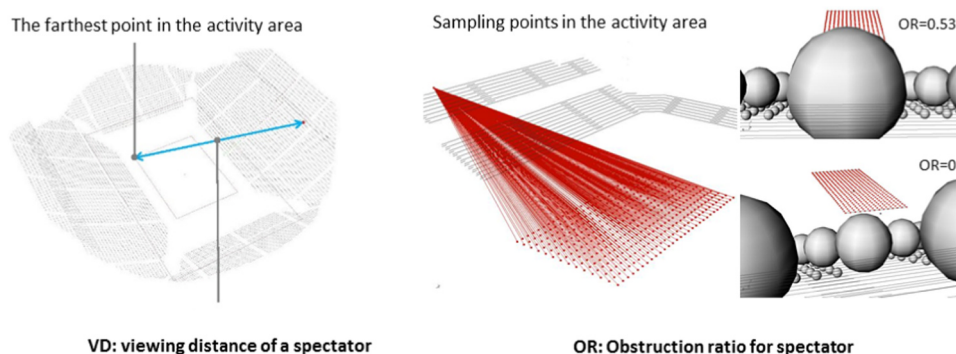

Fig. 8. Measurement of viewing distance (left) and obstruction ratio (right) [16].
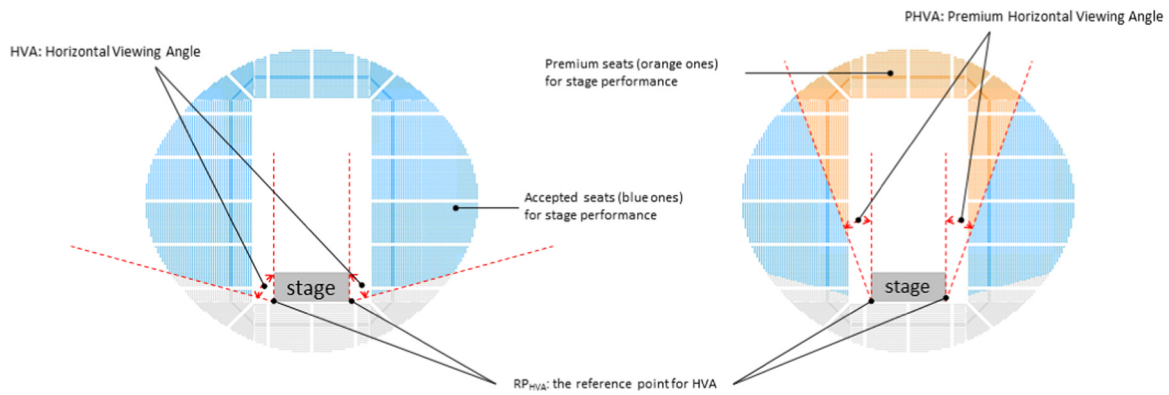
Fig. 9. Defining accepted seats and premium seats for stage performance based on HVA (Horizontal Viewing Angle).

While for the sports competitions, the reverberation time at middle frequencies (around 1 kHz) for an occupied sports venue is required to be between 1.5 and 2.0 s [60,10]. Furthermore, for multi-functional arenas, besides sports events, stage performances (e.g. pop concert) are also important activities which have more strict requirements on reverberation time and should be given priority. Some movable or foldable ceilings are used in theatres and opera houses to meet different requirements, but in sports arenas, such a ceiling is seldom used, since it may influence the functions of other facilities under the roof. Hence, for acoustics, this paper mainly focuses on the requirements of stage performances which require the RT value for specific ranges (Fig. 10).

It is worth noting that without any professional acoustic operation during the early design stage, the reverberation times for most of the design alternatives are usually larger than the required value. Hence, based on stage performances which are considered important for multi-functional arenas, a certain value of RT in Fig. 10 can be selected as a target value to get close to. Alternatively, a range of RT can be set as a design constraint.

3.2.3. Structural performance

For long-span roof structures, as mentioned, the structural mass (SM) and strain energy (SE) are used as indicators [19–21,33,38]. The structural mass (SM) is not directly related to the cost. However, reducing structural mass can save material for structure and reduce the embodied energy which meets the requirements of sustainability [21]. The strain energy of a structure refers to the energy stored within a deformed structure which is bearing loads. To minimize the strain energy means enhancing the structural stiffness [20]. Besides, according to various design codes, to ensure the serviceability of a structure, a series of mechanical indicators should be considered. With the European code EN 1990 [62] and EN 1993-1-1 [63] as examples, the design values of normal stress for each element (σ_{ED}) should be smaller than the allowable stress (σ_{RD}) and the deflection of the overall structure should not be larger than the 1/250 of the span (Dutch national annex of EN-1993-1-1:2005). The values of these two indictors can be also

minimized in the design process to enhance structural performance.

The structural analysis is performed by Karamba 3d [64], a structural analysis plug-in for Rhino-Grasshopper. The structural elements generated by the proposed parametric model are transformed into structural members that can be identified by Karamba 3d, and the material, supports, cross-sectional size, and loads conditions can be assigned by designers.

The setting of the structural analysis in Karamba is listed in Table 4. Specifically, the loads for the structural simulation in this paper include a fixed dead load (except the structural self-weight) of 7 kN/m^2 and live load (snow and wind) of 3 kN/m^2. According to design codes, the snow and wind loads for a roof should be calculated based on the slope angle of the roof. However, for a complex free-form roof, the slope varies in different parts, and the roof geometry also varies during the optimization. Therefore, a complex load model is needed to define the wind and snow loads entirely according to design codes. Alternatively, considering the level of analysis typically used in architectural conceptual design, these loads can be simplified into fully and asymmetric vertical loads for the roof, [21,47]. The lateral load is usually resisted by other structural systems (e.g. vertical elements, shear wall, bracing frames) which are undefined in this design stage and will be defined in the following steps by considering the annex rooms around the multi-functional space.

Although this load model is simplified with the consideration of the level of analysis typically used in architectural conceptual design to search for suitable overall forms, further structural analysis will be performed in the following design stages (Fig. 4). It is worth noting that the load model (Table 4) used in this paper is just one example. Designers are encouraged to use their own load values, loads cases, and load model.

For the structural cross-section, hollow circles are used in this paper. Designers should provide the ranges of the diameter and thickness of hollow circle section. Based on the ranges, proper sizes can be selected by the cross-section optimization embedded in Karamba 3d, which can use less material while satisfying the requirements on the elemental

Table 3
Absorption Coefficient for different areas of sports arenas (selected from Bork, 2005) [59].

| Area	Material	Absorption Coefficient Octave band frequency in Hz						
		125	250	500	1k	2k	4k	8k
Pitch floor	Rubber on concrete	0.02	0.03	0.03	0.03	0.03	0.02	–
Seating tiers floor	Audience floor, 2 layers, 33 mm on sleepers over concrete	0.09	0.06	0.05	0.05	0.05	0.04	–
Walls	Fabric-covered panel, 6 pcf rockwool core	0.21	0.66	1.0	1.0	0.97	0.98	0.98
Spectator area	Audience area, 1 person / m2	0.16	0.29	0.55	0.80	0.92	0.90	–
Ceiling	Metal panel ceiling, backed by 20 mm Sillan acoustic tiles, panel width 85 mm, panel spacing 15 mm, cavity 35 cm	0.59	0.80	0.82	0.65	0.27	0.23	–
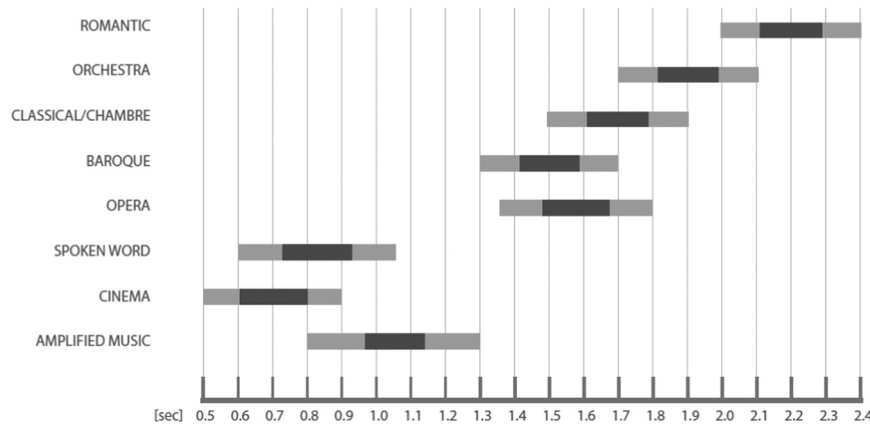
Fig. 10. Requirements on reverberation time of different activities (the dark bars indicate the suitable range and the light ones indicates the acceptable range) [58,61].

stress and strain and the vertical deflection of the whole structure according to the European code EN 1993-1-1 [63]. More detail can be found in the manual of Karamba 3D [65].

According to the analyses above, a proposed framework of assessment criteria for arenas is concluded in Table 5. Designers can formulate specific assessment criteria by selecting different indicators as design objectives and constraints, according to specific design requirements.

3.3. Optimization and post processing

3.3.1. Multi-objective optimization

To start the MOO, design variables (which can be changed during optimization) with related ranges, should be defined based on the parameters in Table 2. Additionally, specific assessment criteria should be formulated as design objectives and constraints, by selecting indicators in Table 5. The 'gamultiobj' function in the optimization toolbox of MATLAB [45] is used to undertake the optimization based on NSGA II [46] as the searching algorithm.

For the diversity of the solutions selected by MOO, an adaptive mutation function is used to define the mutation rate during optimization. By this function, solutions obtaining high scores of fitness functions are given lower mutation rate while the solutions with lower scores are given higher mutation rates [66]. This is performed by the 'mutationadaptfeasible' function of multi-objective optimization toolbox in MATLAB [45].

3.3.2. Hierarchical clustering

Manual classification can be used by designers to group a small number of Pareto solutions according to their geometries (E3 in Fig. 4). If there are too many solutions, clustering analysis can be used to fulfil the task automatically (E4 in Fig. 4).

Clustering analysis (clustering) groups objects into different clusters according to their specific features, and objects in the same cluster are considered to be similar in these features [67]. Such clustering is performed by calculating the distances among objects based on their input data related to the features. A smaller distance between two objects indicates they are more similar. For example, for a certain feature of object a and b, which are respectively indicated by parameters v_{ai} and v_{bi} (for $i = 1$ to n, assuming there are n parameters related to the feature for each object), the distance between object a and b for this feature can be calculated according to Euclidean:

$$d(a, b) = \sqrt{\sum_{i=1}^{n} (v_{ai} - v_{bi})^2} \, \# \tag{5}$$

Other formulas, e.g. Mahalanobis distance, City block distance, Minkowski distance, Chebychev distance, Hamming distance, can be also used to define the distances.

Hierarchical clustering is a clustering method creating a cluster tree or dendrogram. In the bottom level of a hierarchical upside-down tree, each object is seen as an independent cluster, and each cluster connects to others at the higher level to create a bigger cluster, according to the feature distances. Finally, at the top of the tree, all the clusters are connected together [67]. Based on the tree, the similarity between objects in a specific feature is visualized. More details are demonstrated in the sub-Section 4.1.

This paper uses hierarchical clustering to visualize the geometric diversity of the Pareto solutions of optimization. Therefore, the objects of clustering are the Pareto solutions, and the input parameters for the distance calculation is the geometric variables of the Pareto solutions. A feature scaling is used to pre-process the input data for the clustering, to guarantee the accuracy [68]. The 'clusterdata' function of the Statistics and Machine Learning toolbox in MATLAB [45] is used to achieve the hierarchical clustering and formulate the dendrogram.

Table 4
Settings for structural analysis.

Structural element	The grids generated in the parametric model (see step 4 in Table 2) can be automatically transformed into the axes of the elements
Supports	Assigned by designers based on the structural boundary generated in the parametric model
Cross-section	Hollow circles (the ranges of the diameters and thickness are provided by designers, and proper sizes for each solution can be defined by the 'cross-section optimization' in Karamba 3D)
Material	S235, S275, S335
Load	Dead load (except the structural self-weight): 7 kN/m²
	Live load (snow, wind): 3 kN/m²
	Load cases:
	1. dead load (include structural self-weight)
	2. dead load (include structural self-weight) + live load
	3. dead load (include structural self-weight) + asymmetric live load (the asymmetric live load only act on the north, south, east, and west part of the roof, respectively)

Table 5
The proposed framework of assessment criteria.

Aspect	Indicator	Design objective	Design constraint	Related parameters
Accommodation of activities	Types of activities held in the arena	-	-	
Spectators' view	VD_{avr-p}: Average viewing distance for the principal activity	$Min.VD_{avr-p}$	-	Court size of the principal activity for sport event
	VD_{max-e}: The maximum viewing distance of different activities	$Min.VD_{max-e}$	$VD_{max-e} \leq VD_{rec-e}$ [a]	Sizes of courts and stages for all the activities
	RO: The sightline obstructed ratio	$Min.RO$	$RO \leq RO_{rec}$	
	RU: The ratio of useful seats for stage performance	$Max.RU$	$RU \leq Ru_{rec}$	Location of the stage,
	RS_{P-HVA}: the ratio of the seats with premium horizontal viewing angle for stage performance;	$Max.RS_{P-HVA}$	$RS_{P-HVA} \leq RS_{rec}$	Dimension of the stage, RP_{HVA}: Reference point for HVA, HVA: Horizontal viewing angle, P-HVA: Premium horizontal viewing angle.
Acoustics	RT_{60}: Reverberation time	$Min.RT_{60}$	$RT_{60} \in [R]$	Absorption coefficients for different areas (Table 3) Preferred ranges of RT for different activities (Fig. 8)
Structure	M: Structural mass/self-weight	$Mini. M$	$M \leq M_{rec}$	Load Case
	E: Strain energy	$Mini. E$	-	Structural Material
	σ_{max}: the maximum normal stress of elements	$Mini.\sigma_{max}$	$\sigma_{x,Ed} \leq \frac{f_y}{\gamma_M}$ [a]	Sectional dimensions
	d: Vertical deflection	$Min.d$	$d \leq \frac{span}{250}$ [a]	

$d \leq \frac{span}{250}$ is regulated by euro designcode for structure design and Dutch National Annex [63].

[a] $\sigma_{x,Ed} \leq \frac{f_y}{\gamma_M}$ is regulated by euro designcode for steel structure EN 1993-1-1 [63], where f_y is the yield strength related to the material, and γ_M is the Partial factors.

4. Case studies

In this research, the case studies serve two goals: testing the capacity of the proposed parametric model and testing the entire design process. Three arenas, the Barclay Centre, the O2 Arena, and the Philippine Arena, are used for the case studies.

The Barclay Center in New York, U.S. (designed by SHoP Architects PC), which has a symmetric seating bowl, is a typical arena mainly for sports events (basketball games for NBA and Ice hockey games for NHL) and sometimes for pop-music concerts. The O2 Arena in London, U.K. (designed by Populous), which has a seating bowl being asymmetric along the long axis of the pitch (y-axis), is mainly used for both pop-music concerts (with an end-stage or a central stage) and sports events. These two examples represent two of the main categories of arenas all over the world. There is the third kind of arenas, which have seating bowls being asymmetric along the short axes of their pitches (x-axes) and are similar to theatres. The Philippine Arena in Bocaue, Philippine (designed by Populous) is a representative example.

For the testing of the proposed parametric model, the capacity of the model to approximate the geometry of the real buildings is considered. The goal is to assess the capacity of the parametric model to cover a wide range of typologies. To test the parametric model, all three case studies are used. As illustrated in Part C of Figs. 7, 11, and 14, the proposed parametric model is able to generate geometries that approximate all these three arenas, closely enough (according to the pitch size, overall shapes of the seating bowl and the roof) for the early design stage.

For the testing of the entire workflow of the proposed design process, the goal is to assess the capacity of the workflow to support the

design exploration of well performing solutions belonging to different typologies. The process is presented in the following sub-sections and aims also at showcasing how the workflow can be used in design practice. To test the entire workflow, the two most common categories of arenas are selected out of the three: the Barclay Centre and the O2 Arena.

It should be noticed that the selected real arenas are used in order to contextualize realistic backgrounds for the case studies. However, the testing process uses design requirements that may differ from the specific requirements for which the real arenas were designed. This implies the results of the optimizations may be quite different from the original designs. The goal of the testing process does not relate to judgments nor performance assessments on the real designs. The goal focuses on the capabilities of the computational process in order to handle and satisfy a set of given design requirements. The Pareto solutions provided by the optimizations are just well-performing based on these selected requirements.

4.1. The Barclay Centre: an arena mainly for sports events and also sometimes for pop-music concerts

The Barclay Centre (Fig. 11, left and middle) is a typical arena which is mainly for basketball and ice-hockey games and is also sometimes used for pop-music concerts. The seating bowl is symmetric in both long and short directions with 18,700 fixed seats, the plan of the seating bowl is an approximate octagon. The long-span roof is a shallow dome with space-frame structure. A similar solution with a space-frame structure is also in the design space generated by the proposed parametric model (Fig. 11, right), which can be compared with the Pareto
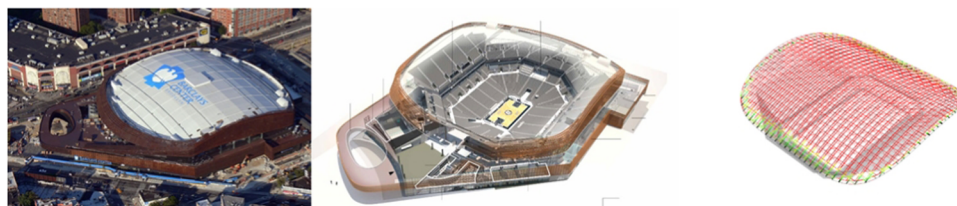
Fig. 11. The Barclay Centre (left and middle) and a similar solution (right) generated by the proposed parametric model (picture sources [54,55]).

Table 6
Input data of the optimization for the Barclay Centre (OPT. 1).

| Objectives	1		min. V_{avr-p} (the maximum value of the average viewing distances of both basketball and ice-hockey)
	2		min. $(RT_{60} - 1.3s)$
	3		min. SM (Structural mass / self-weight)
Constraints	1		The maximum viewing distance for ice-hockey $\leq 110m$
	2		The maximum viewing distance for basketball $\leq 130m$
	3		Fix seats number: $18,000 \leq Seat\text{-}Num \leq 19,000$
	4		The normal stress of structural elemental cross section: $\sigma_{x,Ed} \leq \frac{f_y}{\gamma_M}$, $\gamma_M = 1.25$
	5		Structural vertical deflection: $d \leq \frac{span}{250}$
	6		Other structural constraints (e.g. elemental buckling) according to design code EN 1993-1-1
Parameters	1	P-size	Dimensions of the pitch (ice-hockey): 65m × 36m × 18m
	2	SE_{PRI}	Principal activity for sports event defined by the developer: basketball and ice-hockey
	3	V	C-value: the vertical difference from eyes of a spectator to the top of the head: 120mm.
	4	Dpth-SR	Depth of a seating-row: 0.8m
	5	Width-S	Width of a seat: 0.5m
	6	Nur-SR	Number of the seats between radical or parallel passageways: ≤ 28
	7	Wdth-PW	Width of a passageway: 1.2m
	8	Seat-Sec	Number of the sections of the seating tiers: 3 sections
	9	Row-Sec	Number of rows for each section:
			– lower tiers (without retractable seats): ≤ 12
			– middle tiers: ≤ 18
			– Higher tiers: depends on the boundary
	10*	L-X	Length in X direction: 100m – 160m
	11	Asy-X	Asymmetry in X-axis: 0
	12*	L-Y	Length in Y direction: 90m -120m
	13	Asy-Y	Asymmetry in Y-axis: 0
	14*	Cp-I, Cp-ii, Cp-iii, Cp-iv	Corner positions in 1st, 2nd, 3rd, and 4th quadrant: 0, 1, 2, 3
	15*	Cuv-BO	Curve degree of the building outline: 1 (polyline) and 3 (curve)
	16*	H-CPi-bdr	The height of the ith control point of the structural boundary: 0 to 10
	17*	CenH-roof	headroom of the centre of the pitch: 20m - 45 m
	18*	Cuv-X-roof	Curve degree of the grid in X axis: 1 (polyline) and 3 (curve)
	19*	Cuv-Y-roof	Curve degree of the grid in Y axis: 1 (polyline) and 3 (curve)
	20*	StruDpth-ctr	Structural depth in the centre (for space frame and truss beam): 2m – 6m
	21*	StruDpth-bdr	Structural depth on the boundary (for space frame and truss beam): 0.8-3m
	22*	StruType	Structural type: 0: GS (Grid Shell); 1: SF (space frame); 2: TBX (truss beam along x-axis); 3: TBY (truss beam along y-axis).
	23*	GridSize-roof	Size of the grid: 1.8-2.2 m for Grid-shell 4-5m for space-frame and truss beam
	24*	Cross-section	Circle hollow, diameter: 0.3 - 0.6m, thickness: 20 – 80 mm.
	25	Structure Material	S275

solutions of the optimization.

The optimization for this example is labelled as OPT. 1. Since the Barclay Centre is mainly for basketball and ice-hockey games, the minimization of the maximum value of the average viewing distances for both these two games is set as a design objective to search good seating bowls. Considering it also need to be used for pop-concert, the reverberation time is required to getting close to 1.3 s (the upper boundary of the RT for amplified music, see Fig. 10). It is worth noting that in the primitive design stage for an arena with a large volume, without any professional design for acoustics, the RT value is usually larger than the acceptable values. Therefore, the minimization of the difference between the RT value and 1.3 s is set as the second design objective. For the long-span structure, the minimization of the structural mass is set as the third design objective, aiming at reducing the material consumption and the embodied energy [21]. The details of the input data for the optimization are listed in Table 6. The parameters labelled with '*' in Table 6 are variables which can be changed by the optimizer within the given ranges. The generation number for this optimization is 80 and the population size for each generation is 150. The result is illustrated in Fig. 12. Additionally, besides the manual classification of the Pareto solutions according to geometry, a hierarchical clustering is used to group the Pareto solutions automatically (Fig. 13), which is more efficient in dealing with a large number of solutions.

In part A of Fig. 12, the coordinate chart illustrates the values of the Pareto solutions in the three design objectives. The solutions are represented by the solid dots, and the hollow circles are the projections of the dots on the three planes of the coordinate system. Different colours

of the dots and of the labels of the solutions indicate different structural types: green for grid-shell, blue for space-frame, and red for truss-beam. The left and right columns and the bottom row along the coordinate charts illustrate some key solutions on the Pareto frontiers of obj.1 vs obj.3, obj.2 vs obj.3, and obj.1 vs obj.2, respectively. The solutions here are selected by the authors to study how the geometry and structural type vary with the change of performance values, and the related analyses are listed below. Designers can also explore other Pareto solutions.

1. For the left column, from the solution 22 to 15, as the structural type changes from space-frame to grid-shell, the structural mass gets small, meanwhile, the boundary of the seating bowl gets larger along the short axis of the pitch (x-axis), and the viewing distance getting larger. As the structural mass decreases, from solution 22 to 1 with space-frame structure, the roof changes from flat to convex, and from the solution 21 to 15, with a grid-shell structure, the roof changes from flat to saddle.

2. For the right column, from solution 5 to 15, as the structural mass decreases and the RT increases, the seating bowl changes from rectangle to oval and the roof changes from saddle to concave and saddle again. The solution 5 and 34 share the same shape, but the solution 5 applies one-layer grid-shell structure which is much heavier (with this roof shape) than the two-layer space-frame structure. Meanwhile, for the solution 34, since the two-layer structure, the structural depth increases the height of the roof and then increases the indoor volume and the reverberation time. A similar phenomenon appears between the solution 37 and 12.
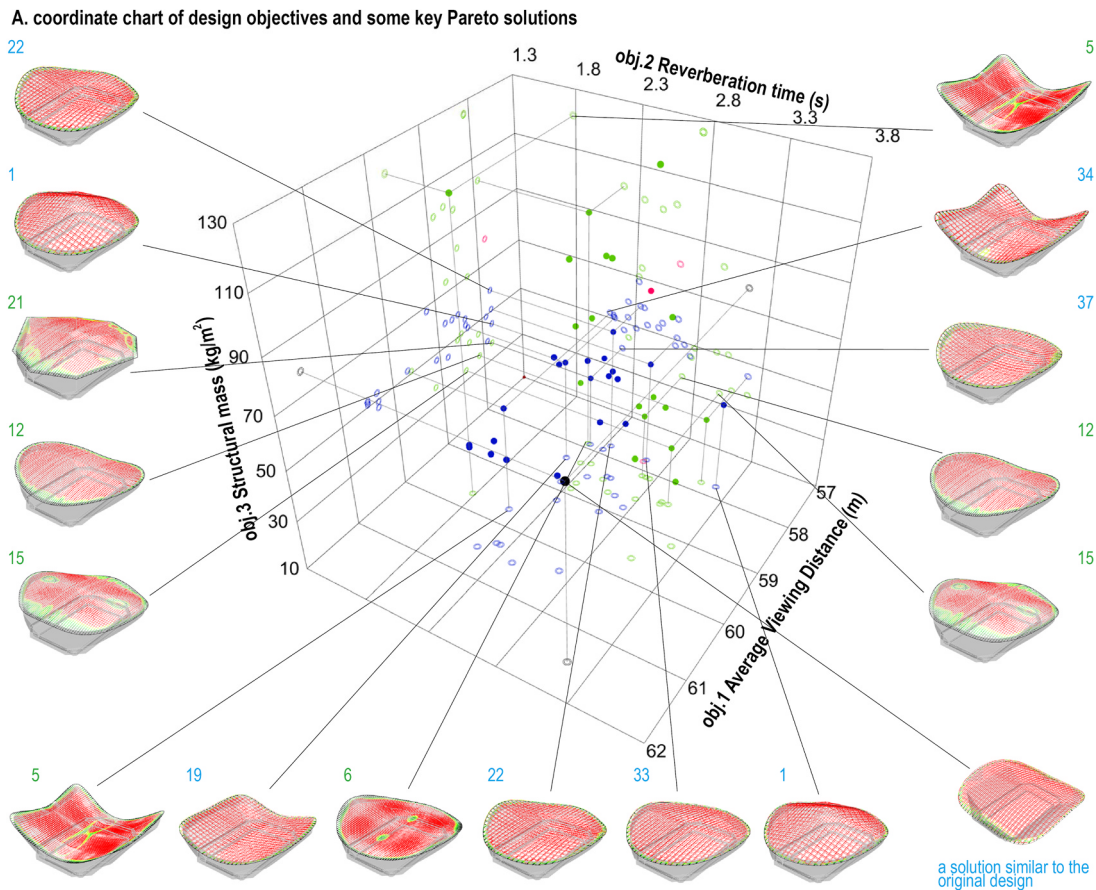
A. coordinate chart of design objectives and some key Pareto solutions

B. Comparision of the pareto solutions, a solutions similart to the original design, and some solutions selected from the iteration history of the optimization.

	a solution similar to the original Pareto Solutions	a	b	c	d	e
Structrual type	-	Space-frame	Grid-shell	Space-frame	Space-frame	Grid-shell	Truss-beam
obj.1 Average viewing distance (m)	57.71- 65.11	63.94	62.59	60.34	62.52	64.96	64.22
obj.2 Reverberation time (s)	1.49 - 2.88	3.84	3.41	3.25	3.62	3.21	2.81
obj.3 Structural mass (kg/m^2)	34.2-125.85	41.07	187.2	66.01	69.27	164.52	59.01

C. Manual classifiction of the Pareto solutions based on geometry

London Velodrome designed by Hopkins
(Photo copyright: Anthony Charlton)
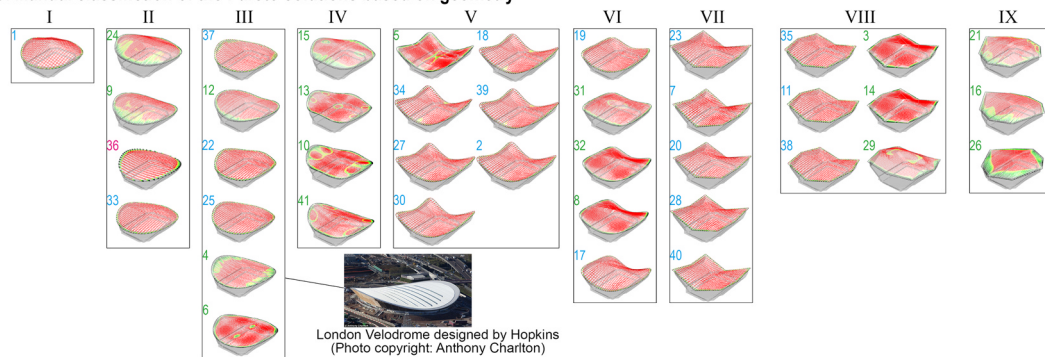
Fig. 12. Results of OPT.1 (solutions with grid-shell, space-frame, and truss-beam structures are labelled in green, blue, and red, respectively) (picture source [69]).

3. For the bottom row, from solution 1 to 5, the seating bowl changes from round to oval and rectangle, which increases the viewing distance. Meanwhile, the roof changes from convex to flat, concave, and saddle, which decreases the volume and decreases the reverberation time.

4. For the solutions with space-frame and truss-beam structures (represented by the blue and red dots, respectively), the structural

weights are small among all the Pareto solutions. For grid-shell solutions, although some obtain smaller weights, most of them are heavy among all the Pareto solutions.

5. The solution similar to the original design is represented by the dark dot in the coordinate chart, which is not so far from the Pareto frontier. Its structural mass is close to the average value of those of the Pareto solutions, while its values of viewing distance and
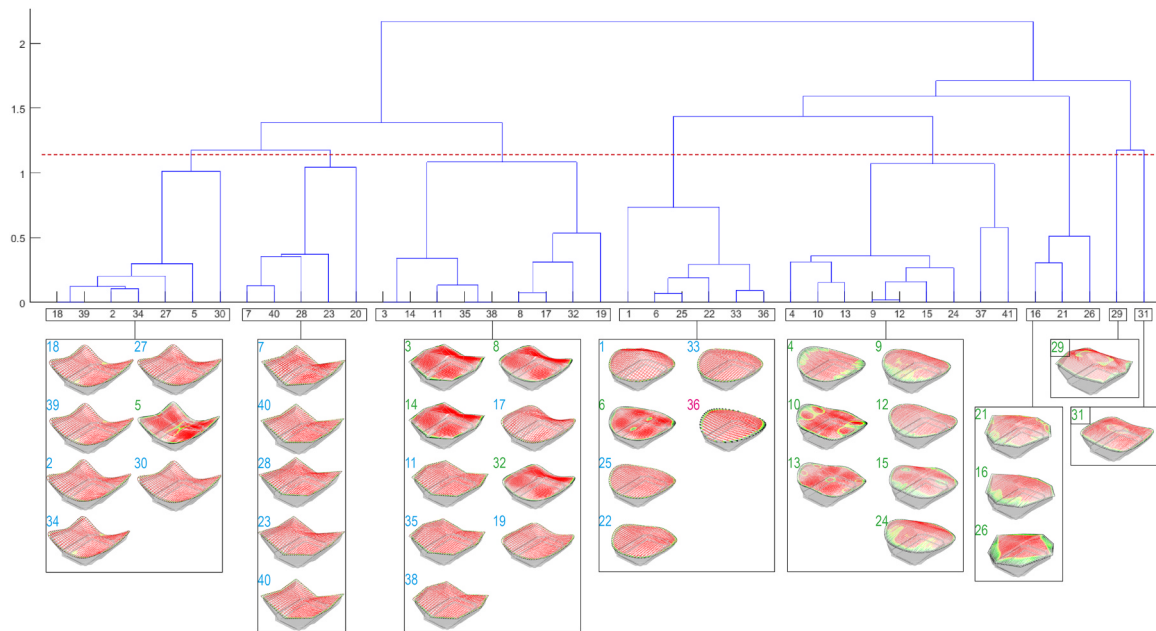
Fig. 13. Hierarchical clustering for the Pareto Solutions of OPT.1 (solutions with grid-shell, space-frame, and truss-beam structures are labelled in green, blue, and red, respectively).

reverberation time are around the upper boundaries of the counterparts of the Pareto solutions.

In part B of Fig. 12, based on the record of the iteration history, some solutions, which are evaluated but eliminated out during the optimization, can be selected by designers to make a comparison with the Pareto solutions according to their performance values. This allows designers to explore more diverse solutions in the design space. The selected examples also demonstrate that besides the Pareto solutions, there are more diverse types of solutions in the design space.

In part C of Fig. 12, all the 41 Pareto solutions are classified manually by the authors according to their judgements on the similarity in geometry, therefore to demonstrate the diversity. Designers can also make a classification based on their judgements. It is worth noting that based on the manual classification, the solutions in the 3rd group are similar to the design of London Velodrome (designed by HOK), which further demonstrates that designers can explore quite different design concepts by the proposed process.

The same grouping work can be also automatically done by hierarchical clustering, especially in dealing with a larger number of solutions (Fig. 13). In this example, the input data for clustering is the variables related to geometry (the variable 10–21 in Table 6). According to the formula (5) in the sub-Section 3.3.2, the Euclidean distances between the solutions will be calculated to identify the similarities. A dendrogram is used to visualize the clustering results. In Fig. 13, all the Pareto solutions are listed along the horizontal axis, similar ones (with less distance) are linked by a 'branch' in a small distance (indicated by the vertical axis). Designers can select a certain level of the distance to cut the tree and obtain a certain number of

clusters. In the example of Fig. 13, the tree is cut at the level around 1.2 and is divided into 8 branches (clusters).

4.2. The O2 Arena: an arena for both pop-music concerts and sports events

The O2 Arena (Fig. 14, left and middle) is used for both pop-music concerts and sports events. According to the statistics of 'Pollstar' (a trade industry journal), the O2 Arena was the busiest venue for concerts all over the world in 2016 [70]. Meanwhile, the O2 Arena is also used for various high-level sports events, including some oversea games of NBA (basketball) and NHL (ice-hockey), tennis matches of ATP, and some matches of 2012 summer Olympic games (basketball, artistic gymnastics, trampoline).

With an end stage in the pitch, the rectangle seating bowl of O2 Arena is asymmetric along the long axis of the pitch (y-axis), therefore most of the fixed seats are available for stage-performance. Although the venue is covered by the famous Millennium Dome, it has an independent roof with space-frame structure (composed by two main trusses and many small trusses) [71]. Therefore, in this paper, it is considered as an independent venue without the membrane dome. A similar solution (Fig. 14, right) in the design space can be used to compare with the Pareto solutions of the optimization.

Since in practice, designers usually set different combinations of design objectives according to their judgments on the design conditions, and it is worth studying how the results will change based on different optimizations for one scenario. Hence, two design optimizations with different objectives are used to guide the design exploration. The first optimization (OPT. 2-A) is based on the same objectives with those in the sub-Section 4.1 (OPT. 1). One additional constraint is
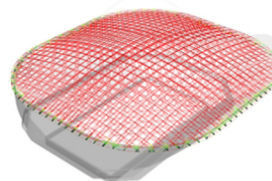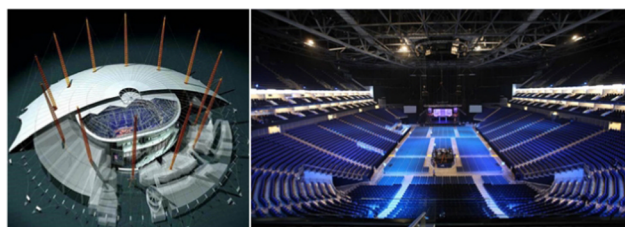
Fig. 14. The O2 Arena (left and middle) and a similar solution (right) generated by the proposed parametric model (picture sources [72,73]).

Table 7
Input data of the optimization for the O2 Arena (OPT.2).

OPT. 2-A	Objectives	1	min. V_{avr-p} (the maximum value of the average viewing distances of basketball)	
		2	min. (RT_{60} -1.3s)	
		3	min. SM (Structural mass / self-weight)	
	Constraints	1	Ratio of multi-functional seats: RU$\geq$ 85% (HVA = 90 degrees, end stage size: 25m × 10m, the reference points are the back corners of the stage)	
		2	Fix seats number: 19, 000$\leq$Seat-Num$\leq$ 21,000	
			The other constraints are the same with those of OPT.1 in Table 6	
OPT. 2-B	Objectives	1	max. RS_{P-HVA} (the ratio of seats with a premium horizontal angle, P-HVA = 20 degrees) for seats in the upper tiers	
		2	min. (RT_{60} -1.3s)	
		3	min. Strain energy of the roof structure	
	Constraints		The constraints are the same with those of the Opt. 2-A.	
Parameters for both OPT. II-A and OPT. II-B		1	P-size	Dimensions of the pitch: 40m × 70m
		2	SE_{PRI}	Principal activity for sports event: basketball
		3[a]	Asy-Y	Asymmetry in Y-axis: 6 to 10
		4[a]	Cp-I, Cp-ii,	Corner positions in 1st, 2nd, 3rd, and 4th quadrant
			Cp-iii, Cp-iv	Cp-i = Cp-iv: 0 to 3; Cp-ii = Cp-iii: 0 to 3.
			Other settings of variables are the same with the optimization I in Table 6.	

[a] The labelled parameters are variables which can be changed by the optimizer within the given ranges

added to meet the background of the O2 Arena, which requires 85% of the fixed seats to be available for the performance with an end-stage. The second optimization (OPT. 2-B) aims at maximizing the RS_{P-HVA} (the ratio of seats with premium horizontal viewing angle) for the fixed seats in the upper tiers, to increase the number of the seats within a good viewing range of stage-performance. It also aims at minimizing the reverberation time which is the same as the first optimization and minimizing the strain energy of the structure to increase the stiffness. The inputs for these optimizations are listed in Table 7. The results of the two optimizations are illustrated in Figs. 15 and 16, respectively.

For the part A in Fig. 15, there are some observations about the results of the OPT.2-A.

1. For the left column, from solution 5 to 3, as the shape of the seating bowl changes from an approximate round to a shape like a chestnut (which is round at one end but has a cusp at the other end), and also as the roof changes form concave to convex, the viewing distance increases and the structural mass decreases. Solutions 5 and 7 have similar shapes, and the viewing distances are the same, but the space-frame structure (solution 7) is lighter than the grid-shell (solution 5).

2. For the right column, from solution 40 to 3, as the reverberation time increases and the structural mass decreases, the shape of seating bowl varies randomly but the roof changes from concave to convex.

3. For the bottom row, from the solution 7 to 40, the shape of the seating bowl changes from an approximate round to a chestnut shape, a rectangle, and a trapezoid, which increases the viewing distance. Meanwhile, as the increase of the curvature for the concave roof, the reverberation time decreases. The solution 7 and 5 share the same geometries and have the same value in viewing distances (as mentioned in the first observation), but the solution 7 use space-frame and its roof is higher since its structural depth which increases the indoor volume, therefore, increases the reverberation time.

4. Similar to the result of the OPT.1, the space-frame and truss-beam solutions have small structural mass, among all the Pareto solutions.

For grid-shell solutions, some obtain much smaller weights while most of them are heavy among all the Pareto solutions. Comparing with those of the OPT.1, the Pareto solutions of the OPT.2-A have more truss-beam solutions.

5. For the similar solution to the original design, its values related to the three objectives are larger than most of the Pareto solutions.

For the part A in Fig. 16, some observations about the OPT.2-B are provided by the authors, which are quite different from the counterparts of OPT.2-A, since the different design objectives.

1. For the left column, from the solution 1 to 4, with the decrements of both RS_{P-HVA} (ratio of seats with premium horizontal viewing angle) and strain energy, the overall geometry changes from a shape like a slope to a chestnut shape. The solutions 1 and 24 obtain a high score in RS_{P-HVA} since most of the seats of the upper tiers face the frontage of the stage and with a good horizontal viewing angle (see the objective 1 for OPT.2-B in Table 7), these two solutions share similar geometries, but the strain energy of the solution 24 with truss beam is much less than that of the solution 1 with grid-shell structure.

2. For the right column, from the solution 18–4, as the strain energy decreasing and the reverberation time increasing, the geometry changes form a rectangle seating bowl with a concave roof to a trapezoid seating bowl with a saddle roof and a chestnut shape geometry with a convex roof (which is similar to the last two solutions in the left column).

3. For the bottom row, from the solution 1–13, all the roofs are concave and all the seating bowls are rectangles, but as the length of the seating bowl along the long axis of the pitch shortening, the number of seats in front of the stage decrease, therefore, the RS_{P-HVA} also decrease. This transformation also reduces the indoor volume then decreases the reverberation time.

4. For the structural types of the Pareto solutions, there are two obviously clusters of dots in the coordinate chart, which is different from the results of the previous two optimizations. One is composed by all green dots (solutions with grid-shell structure) and is in the upper left of the chart, which means the grid-shell solutions have large values in strain energy but small values in reverberation time. The other cluster is composed by red and blue dots (solutions in truss-beam and space-frame, respectively) and is in the bottom right of the chart, which means these solutions have small values in strain energy and large values in reverberation time. Moreover, the number of truss-beam solutions increases a lot comparing to the other two optimizations.

5. The solution similar to the original design (represented by the black dot) is far from the Pareto frontier. Comparing with the values of the Pareto solutions, its RS_{P-HVA} value is on the average level, while its values in both strain energy and reverberation are quite large.

In the OPT.2-A and OPT.2-B, some other diverse solutions are present in the design space, but are eliminated by the optimizations. They can be also explored and compared with the Pareto solutions based on geometries and performance values (Figs. 15B and 16B).

The parts C of both Figs. 15 and 16 respectively illustrate the manual classifications of the Pareto Solutions from the two optimizations (OPT. 2-A and OPT. 2-B, which have the same variables and constraints but different objectives). Some types of geometries are selected by both optimizations, but in OPT. 2-B, there are some special types (e.g. the types I to V in part C of Fig. 16). Some of the geometries are also similar to some real arenas. The geometries of the types V, VI, and VII in part C of Fig. 15 are similar to the London aquatics centre (designed by Zaha Hadid) with its temporary seating tiers. The geometries of the types I, II, and III in part C of Fig. 16 are similar to the Barcelona arena (designed by HOK). This demonstrates again, how the proposed design process can facilitate designers to explore different design concepts.
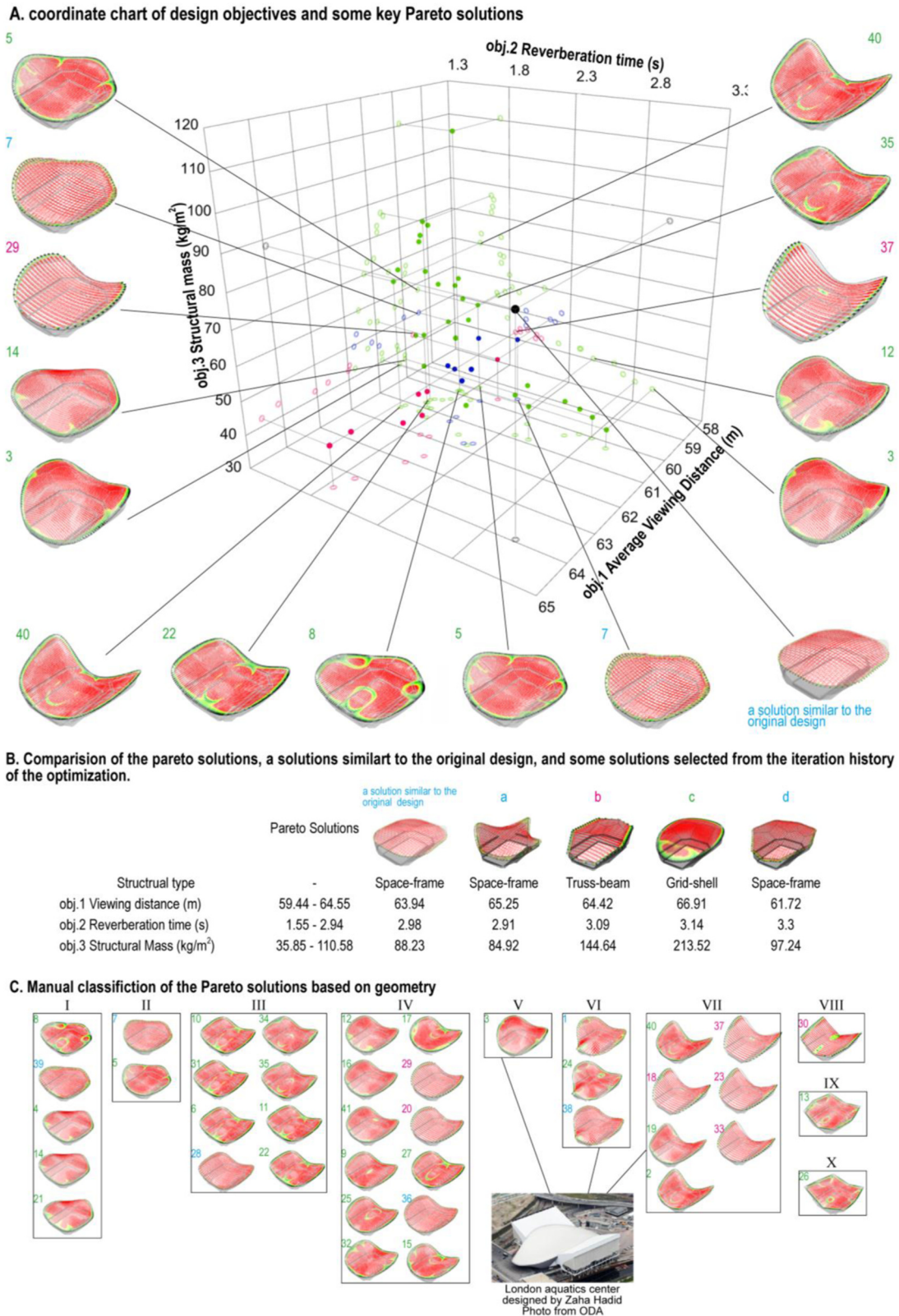
Fig. 15. Results of OPT. 2-A (solutions with grid-shell, space-frame, and truss-beam structures are labelled in green, blue, and red, respectively) (picture source [74]).

5. Discussion

The case studies demonstrate how the proposed design process can be used in practice. In fact, besides the analyses in the case studies, there are various ways to study the relationships among geometries, structural types, and the selected performance by the proposed design process.

The analyses of the results provided by the authors demonstrate the effects of the proposed design process. Based on the analyses, some summaries are listed below:
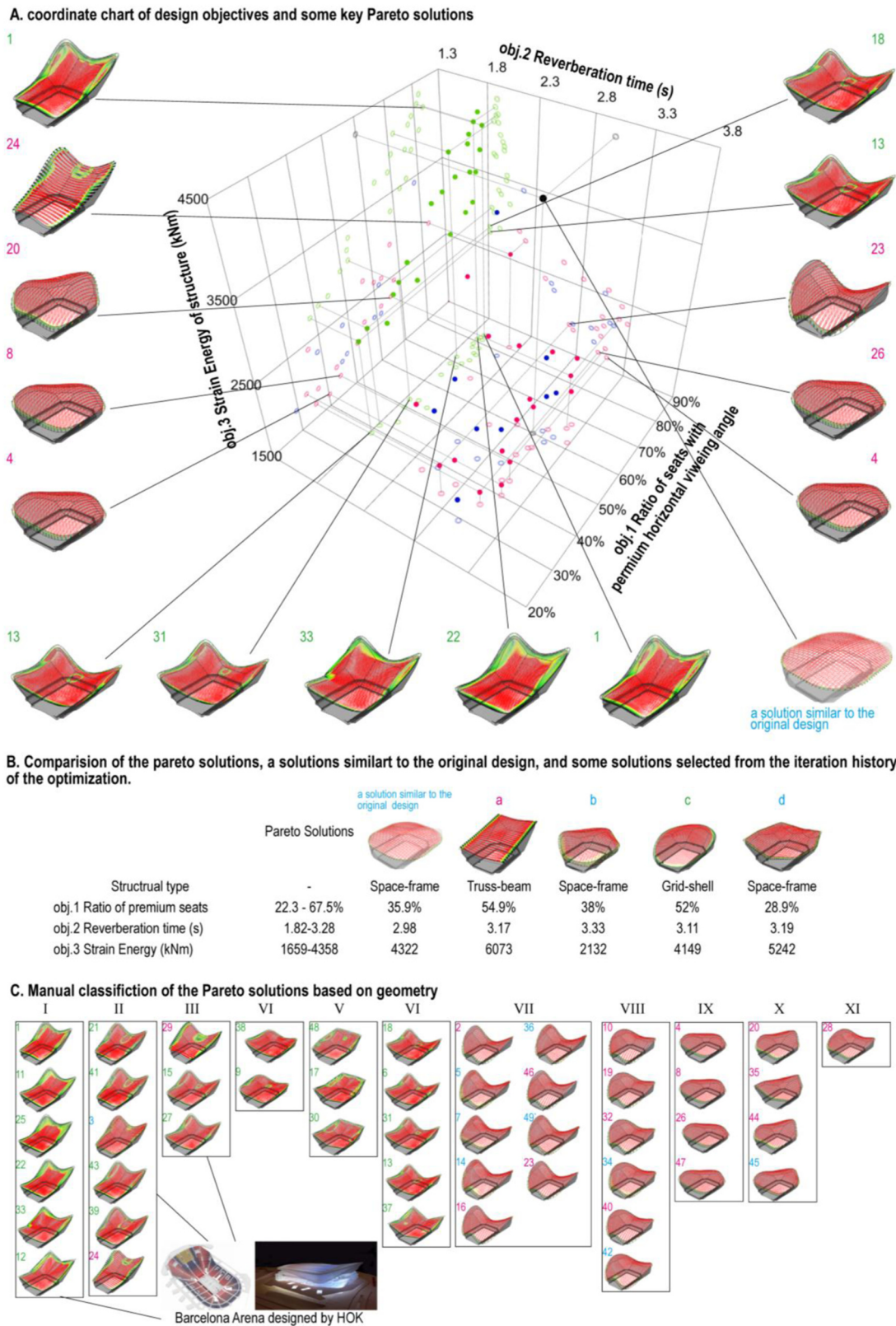
A. coordinate chart of design objectives and some key Pareto solutions

B. Comparision of the pareto solutions, a solutions similart to the original design, and some solutions selected from the iteration history of the optimization.

	Pareto Solutions	a solution similar to the original design	a	b	c	d
Structrual type	-		Space-frame	Truss-beam	Space-frame	Grid-shell	Space-frame
obj.1 Ratio of premium seats	22.3 - 67.5%		35.9%	54.9%	38%	52%	28.9%
obj.2 Reverberation time (s)	1.82-3.28		2.98	3.17	3.33	3.11	3.19
obj.3 Strain Energy (kNm)	1659-4358		4322	6073	2132	4149	5242

C. Manual classification of the Pareto solutions based on geometry

Barcelona Arena designed by HOK

Fig. 16. Results of OPT. 2-B (solutions with grid-shell, space-frame, and truss-beam structures are labelled in green, blue, and red, respectively) (picture source [75,76]).

1. Different design objectives, constraints, and design conditions re-quire different geometries, therefore, providing diverse geometries is necessary and can meet the design requirements better.

  – Different objectives prefer different types of geometries during op-timization. In all the three optimizations, the recurring observations about the key solutions on the Pareto frontiers demonstrated that the geometries transform to different typologies with the decre-ments or increments of the objective values.
  – With the same combination of design objectives, different settings of constraints and variables lead to different geometries in the Pareto solutions. OPT. 1 and OPT.2-A, share the same objectives, but the variables and constraints are different. As a result, although some Pareto solutions of these two optimizations are similar, there are special geometries which only appear in one of the optimizations.
  – With the same setting of constraints and variables, different design objectives also lead to different geometries in Pareto solutions. For the OPT. 2-A and the OPT.2-B, some Pareto solutions of these two optimizations are similar, there are special types of geometries which only appear in one of the optimizations.

2. Providing multiple structural types is necessary for the optimiza-tions related to structures.

  – In all the three optimizations, all of the three structural types appear in the Pareto solutions. For each optimization, the structural per-formance varies for different structural types of the Pareto Solutions. For each structural type, the numbers of Pareto solutions of the three optimizations are also different.
  – With the same geometry, different structural types obtain different values in structural performance. For the key Pareto solutions ana-lysed in Section 4, several pairs of solutions share the same geo-metries but with different structural types, which lead to different values in structural performance (mass or strain energy).

3. The broader design space with diverse geometries not only provides more types of solutions for designers to explore and to compare with the existed design concepts (the solutions similar to the original designs in the examples) but also enlighten designers by the design concepts of other real arenas.

  – The geometries of some Pareto solutions remind of other real arenas, which demonstrates that by using the proposed design process, de-signers can explore other design concepts that they may not think about at the beginning. Some examples of the connections between some Pareto solutions and the real arenas are provided in Section 4. More similar connections can be performed by comparing the Pareto solutions with more real arenas.

4. Performance-driven optimization is a reasonable and efficient way to guide the design exploration of diverse solutions, but it confines the exploration to the well-performing solutions and excludes other solutions in the design space. Some methods need to be developed to support the exploration based on geometric typology, which is also crucial for architectural design.

  – More diverse types of geometries are included in the design space, and just a small part of them are selected by the optimizations as the Pareto solutions. The examples displayed in part B of Fig. 7 de-monstrate the diverse geometries in the broad design space. The examples in part B of Figs. 12, 15, and 16, which select some so-lutions weeded out during the optimizations, also demonstrate that there are various geometries (in the design space) differing from the Pareto ones.

Therefore, for the design optimizations of sports arenas, which focus on integration of multi-functional space and long-span structure in the early design stage, it is crucial to provide solutions with diverse geo-metries and multiple structural types, since different design conditions and assessment criteria require different geometries and it is necessary to explore various possibilities at the early design stage. Furthermore, because it is difficult to predict the considerations of designers in practice, the proposed framework of assessment criteria with different indicators, rather than a set of specific criteria, is necessary.

6. Conclusion

This paper proposes a design process for the early design stage of sports arenas, integrating the multi-functional space and long-span structure, with emphasis on the diversity of alternatives for the design exploration guided by performance-based multi-objective optimization according to various indicators. The proposed process is for the archi-tectural design exploration during the early design stage to define proper overall geometries for the following design stages. Designers can select the aspects of interest to guide the exploration, but specific and professional designs for these aspects cannot be replaced and should be done based on the solutions defined by this design process.

However, there are still some limitations. First, the structural types included in the parametric model are limited and more frequently-used types need to be considered. Second, the topological pattern of the structures is fixed in the model, more patterns or even topology opti-mization can be added. Third, the load model of the structural simu-lations can be improved to adapt to more complex conditions. Fourth, comparing with the manual classification of the Pareto solutions ac-cording to geometry, the results of hierarchical clustering are not ac-curate enough, which may be related to the complexity relationships between the input parameters. Fifth, there are more diverse solutions in the design space but are weeded out by optimization. However, it does not mean they are unworthy for the design. Methods which can facil-itate designers to explore the design space based on not only perfor-mance but also geometric typology is necessary, and clustering is a potential one.

Based on these limitations, future work will focus on two aspects. First, adding the types and topological patterns of structure for the parametric model and improving the load model. Second, study how to use clustering to facilitate designers to explore the design space ac-cording to geometry, and how to improve the clustering results ac-cording to designers' judgements on similarity.

Acknowledgement

References

[1] S. Sariyildiz, Performative computational design, in: Proc. ICONARCH-I Int. Congr. Archit., Selcuk University, Konya, 2012, pp. 313–344.

[2] J. Harding, Meta-parametric Design: Developing A Computational Approach for Early Stage Collaborative Practice, University of Bath, 2014, ⟨https://researchportal.bath.ac.uk/en/publications/meta-parametric-design-developing-a-computational-approach-for-ea⟩.

[3] D.J. Gerber, S.E. Lin, B.P. Pan, A.S. Solmaz, Design optioneering: multidisciplinary design optimization through parameterization, domain integration and automation

of a Genetic Algorithm, in: Symp. Simul. Archit. Urban Des, 2012, pp. 23–30.

[4] M. Turrin, Performance Assessment Strategies: A Computaional Framework for the Conceptual Design of Large Roofs, Delft University of Technology, 2014, ⟨https://books.bk.tudelft.nl/index.php/press/catalog/book/269⟩.

[5] CEN(European Committee for Standardization), EN 13200: Spectator Facilities (Part 1: General characteristics for spectator viewing area), 2012.

[6] R. Hudson, Strategies for Parametric Design in Architecture: An Application of Practice Led Research, University of Bath, 2010, ⟨https://researchportal.bath.ac.uk/en/publications/strategies-for-parametric-design-in-architecture-an-application-o⟩.

[7] Y. Sun, L. Xiong, P. Su, Grandstand Grammar and its Computer Implementation, in: ECAADe 31, 2013: pp. 645–654.

[8] ARUP, STAG:Stadium Generator ,2014. ⟨https://www.arup.com/expertise/services/buildings/architecture⟩.

[9] C. Binkley, P. Jeffries, M. Vola, Design computation at Arup, in: T. Spiegelhalter, A. Andia (Eds.), Post-Parametric Autom. Des. Constr. Artech House Publishers, London, 2014, pp. 112–120.

[10] SportsEngland, Sports Halls Design and Layouts (Updated and Combined Guidance), 2012. ⟨https://www.sportengland.org/media/4330/sports-halls-design-and-layouts-2012.pdf⟩,.

[11] IAEE, Guidelines for Display Rules and Regulations, 2014. ⟨www.mromarketing.aviationweek.com/downloads/mro2017/ERC_Documents/Documents/17_Am_IAEEguidelines.pdf⟩.

[12] N. Miller, Parametric Strategies in Civic Architecture Design, in: ACADIA 09 ReForm - Build. a Better Tomorrow, 2009, pp. 144–152.

[13] R. Hudson, Frameworks for Practical Parametric Design in Architecture, in: Proceedings of the 26th ECAADe Conference: 2008: pp. 847–854.

[14] R. Hudson, P. Shepherd, D. Hines, Aviva Stadium: a case study in integrated parametric design, Int. J. Archit. Comput. 9 (2011) 187–204, https://doi.org/10.1260/1478-0771.9.2.187.

[15] D. Holzer, Y. Tengono, S. Downing, Developing a framework for linking design intelligence from multiple professions in the aec industry, in: Proceedings of the 12th International CAAD Conference, 2007, pp. 303–316. doi:⟨http://dx.doi.org/10.1007/978-1-4020-6528-6⟩.

[16] L. Xiong, W. Pan, Y. Sun, Integrated computational optimization for the layout of the playing hall in the gymnasium based on viewing quality analysis, in: Proc. 2015 Symp. Int. Assoc. Shell Spat. Struct., IASS, Amsterdam, 2015.

[17] R. Hudson, M. Westlake, Simulating human visual experience in stadiums, in: Proc. Symp. Simul. Archit. Urban Des, 2015, pp. 164–171. ⟨http://dl.acm.org/citation.cfm?Id=2873021.2873044⟩.

[18] L.L. Beranek, Music, acoustics, and architecture, Bull. Am. Acad. Arts Sci. 45 (1992) 25–46.

[19] P. von Buelow, Paragen-performative exploration of genetive systems, J. IASS 53 (2012) 271–284.

[20] C.Y. Cui, B.S. Jiang, A morphogenesis method for shape optimization of framed structures subject to spatial constraints, Eng. Struct. 77 (2014) 109–118, https://doi.org/10.1016/j.engstruct.2014.07.032.

[21] N.C. Brown, C.T. Mueller, Design for structural and energy performance of long span buildings using geometric multi-objective optimization, Energy Build. 127 (2016) 748–761, https://doi.org/10.1016/j.enbuild.2016.05.090.

[22] G.P. Hammond, C.I. Jones, Embodied energy and carbon in construction materials, in: Proc. Inst. Civ. Eng. - Energy:, 2008, pp. 87–98. doi:⟨http://dx.doi.org/10.1680/ener.2008.161.2.87⟩.

[23] C. Barrios, Transformations on parametric design models: a case study on the Sagrada Familia columns instances of a parametric model, in: B. Martens, A. Brown (Eds.), CAAD Futur. Springer, 2005, pp. 393–400.

[24] A.T. Nguyen, S. Reiter, P. Rigo, A review on simulation-based optimization methods applied to building performance analysis, Appl. Energy 113 (2014) 1043–1058, https://doi.org/10.1016/j.apenergy.2013.08.061.

[25] S. Amaran, N.V. Sahinidis, B. Sharda, S.J. Bury, Simulation optimization: a review of algorithms and applications, Ann. Oper. Res. 240 (2016) 351–380, https://doi.org/10.1007/s10479-015-2019-x.

[26] M. Hamdy, A. Hasan, K. Siren, Applying a multi-objective optimization approach for Design of low-emission cost-effective dwellings, Build. Environ. 46 (2011) 109–123, https://doi.org/10.1016/j.buildenv.2010.07.006.

[27] M. Fesanghary, S. Asadi, Z.W. Geem, Design of low-emission and energy-efficient residential buildings using a multi-objective optimization algorithm, Build. Environ. 49 (2012) 245–250, https://doi.org/10.1016/j.buildenv.2011.09.030.

[28] R. Evins, A review of computational optimisation methods applied to sustainable building design, Renew. Sustain. Energy Rev. 22 (2013) 230–245, https://doi.org/10.1016/j.rser.2013.02.004.

[29] I. Keough, D. Benjamin, Multi-objective optimization in architectural design, in: 2010 Spring Simul. Multiconference, SpringSim'10, 2010, p.191. doi:⟨http://dx.doi.org/10.1145/1878537.1878736⟩.

[30] M. Turrin, P. Von Buelow, A. Kilian, R. Stouffs, Performative skins for passive climatic comfort: a parametric design process, Autom. Constr. 22 (2012) 36–50, https://doi.org/10.1016/j.autcon.2011.08.001.

[31] X. Shi, W. Yang, Performance-driven architectural design and optimization technique from a perspective of architects, Autom. Constr. 32 (2013) 125–135, https://doi.org/10.1016/j.autcon.2013.01.015.

[32] S.E. Lin, D.J. Gerber, Designing-in performance: a framework for evolutionary energy performance feedback in early stage design, Autom. Constr. 38 (2014) 59–73, https://doi.org/10.1016/j.autcon.2013.10.007.

[33] C.T. Mueller, J.A. Ochsendorf, Combining structural performance and designer preferences in evolutionary design space exploration, Autom. Constr. 52 (2015) 70–82, https://doi.org/10.1016/j.autcon.2015.02.011.

[34] D. Yang, Y. Sun, S. Sariyildiz, Y. Sun, Sports building envelope optimization using Multi-objective Multidisciplinary Design Optimization (M-MDO) techniques, in: 2015 IEEE Congr. Evol. Comput. CEC 2015 - Proc., 2015, pp. 2269–2278. doi:⟨http://dx.doi.org/10.1109/CEC.2015.7257165⟩.

[35] D. Yang, Y. Sun, M. Turrin, P. Von Buelow, J. Paul, Multi-objective and multi-disciplinary design optimization of large sports building envelopes : a case study., in: Proc. 2015 Symp. Int. Assoc. Shell Spat. Struct., IASS, Amsterdam, 2015.

[36] D. Yang, S. Ren, M. Turrin, S. Sariyildiz, Y. Sun, Multi-disciplinary and multi-objective optimization problem re-formulation in computational design exploration: a case of conceptual sports building design, Autom. Constr. 92 (2018) 242–269, https://doi.org/10.1016/j.autcon.2018.03.023.

[37] M. Turrin, D. Yang, A. D'Aquilio, R. Sileryte, Y. Sun, Computational design for sport buildings, Procedia Eng. 147 (2016) 878–883, https://doi.org/10.1016/j.proeng.2016.06.285.

[38] P. von Buelow, Genetically enhanced parametric design in the exploration of architectural solutions, Struct. Archit. (2016) 675–683, https://doi.org/10.1201/b20891-93.

[39] J. Harding, C. Brandt-Olsen, Biomorpher: interactive evolution for parametric design, Int. J. Archit. Comput. 16 (2018) 144–163, https://doi.org/10.1177/1478077118778579.

[40] K. Shea, R. Aish, M. Gourtovaia, Towards integrated performance-driven generative design tools, Autom. Constr. 14 (2005) 253–264, https://doi.org/10.1016/j.autcon.2004.07.002.

[41] H. Engel, Structure systems.pdf, Hatje Cantz Verlag, Berlin, 2007.

[42] S. Dong, Y. Zhao, D. Xing, Application and development of modern long-span space structures in China, Front. Struct. Civ. Eng. 6 (2012) 224–239, https://doi.org/10.1007/s11709-012-0166-6.

[43] Robert McNeel & Associates, Rhinocerous, (n.d.). ⟨www.rhno3d.com⟩.

[44] Robert McNeel & Associates, grasshopper, (n.d.). ⟨http://www.grasshopper3d.com⟩.

[45] The Mathworks, Inc., MATLAB and Optimization Toolbox, (n.d.). ⟨www.mathworks.com/products/matlab.html⟩.

[46] K. Deb, A. Pratap, S. Agarwal, T. Meyarivan, A fast and elitist multiobjective genetic algorithm: NSGA-II, IEEE Trans. Evol. Comput. 6 (2002) 182–197, https://doi.org/10.1109/4235.996017.

[47] J. Kim, H. Ryu, D. Cho, K. Song, Structural design of Philippine Arena, J. Civ. Eng. Archit. 10 (2016) 405–416, https://doi.org/10.17265/1934-7359/2016.04.002.

[48] STRAFP/GettyImagines, The Beijing University of Technology Gym, 2008. ⟨https://www.gettyimages.indetailnews-photothe-beijing-university-of-technology-gymnasium-is-seen-in-news-photo82058078⟩.

[49] ABC, Beijing University of Technology Gymnasium, 2008.

[50] Wikipedia, Arena do Futuro, 2015. ⟨https://en.wikipedia.orgwikifuture_arena#mediaFileArena_do_Futuro_Rio_2016.jpg.pdf⟩,.

[51] YASUYOSHI CHIBAAFP/Getty Images, OLY-2016-RIO-HANDBALL-FUTURE ARENA, 2016. ⟨https://www.gettyimages.nl/detail/nieuwsfotos/general-view-of-inside-the-future-arena-at-the-olympic-nieuwsfotos/539264166⟩,.

[52] Architectuur Centrum Amsterdam, Ziggo Dome, 2014. ⟨https://www.arcam.nlenziggo-dome-2map⟩.

[53] Archdaily, Ziggo Dome Plan, 2014. ⟨https://www.archdaily.com/350923/ziggo-dome-benthem-crouwel-architects⟩,.

[54] Info-stade, Brooklyn Barclay Center, 2013. ⟨http://www.info-stades.fr/stade/418/new-york-brooklyn-barclays-center⟩.

[55] Advance Graphics, Barclay Center Collage - Planaxon, 2015. ⟨https://stblaney.wordpress.com20150115barclay-center-collage⟩,.

[56] STARaGARA.NET, Philippine arena, 2014. ⟨http://www.staragara.net201407jaw-dropping-facts-on-inc-philippine-arena.html⟩.

[57] Gist, Philiarena, 2017. ⟨https://gistph.com20170628how-much-are-purpose-tour-mnl-tickets⟩,.

[58] M. Barron, Auditorium Acoustics and Architectural Design, 2nd ed., Spon Press, London and New York, 2010.

[59] I. Bork, Report on the 3rd round robin on room acoustical computer simulation - Part II: calculations, Acta Acust. U. Acust. 91 (2005) 753–763.

[60] R. Hammad, The acoustics of the amman sport arena the design and result, Archit. Sci. Rev. 43 (2000) 183–189, https://doi.org/10.1080/00038628.2000.9696906.

[61] M. Soru, A Spatial Kinetic Structure Applied to an Active Acoustic Ceiling for A Multipurpose Theatre, Delft University of Technology, 2014.

[62] CEN(European Committee for Standardization), EN-1990: Basis of Structural Design, 2002.

[63] CEN(European Committee for Standardization), EN 1993: Design of steel structures (Part 1-1: General rules and rules for buildings), 2005.

[64] C. Preisinger, M. Heimrath, Karamba - A toolkit for parametric structural design, Struct. Eng. Int. J. Int. Assoc. Bridg. Struct. Eng. 24 (2014) 217–221, https://doi.org/10.2749/101686614X13830790993483.

[65] C. Preisinger, Parametric Structural Modelling (Karamba) User Manual for Version 1.2.2, 2016, pp. 1–142. ⟨http://www.karamba3d.com/downloads/⟩.

[66] M. Srinivas, L.M. Patnaik, Adaptive probabilities of crossover and mutation in Genetic Algorithms, IEEE Trans. Syst. Man Cybern. 24 (1994) 656–667, https://doi.org/10.1109/21.286385.

[67] A. Saxena, M. Prasad, A. Gupta, N. Bharill, O. Prakash, A review of clustering techniques and developments, Neurocomputing 267 (2017) 664–681, https://doi.

org/10.1016/j.neucom.2017.06.053.

[68] C. Yang, B. Wan, X. Gao, Selections of data preprocessing methods and similarity metrics for gene cluster analysis, Prog. Nat. Sci. 16 (2006) 2006.

[69] Anthony Charlton/Daily Mail, the Eagerly Anticipated Olympic, 2011. velodrome. ⟨https://www.dailymail.co.uk/news/article-1359410/London-2012-Olympics-Velodrome-venue-finished.html⟩,.

[70] Pollstartpro.com, 2016 Mid-Year Worldwide Ticket Sales Top200 Arena Venuses, 2016.

[71] NSC2, SSDA 2008 – The O2 Arena, North Greenwich July 1, 2008, ⟨http://www.newsteelconstruction.com/wp/ssda-2008-the-o2-arena-north-greenwich⟩.

[72] trips2London, The O2 Arena London, 2014. ⟨http://www.trips2london.comthe_o2_arena_london.html⟩.

[73] Wikipedia, O2 Arena Hosting a Tennis Match, 2016. ⟨https://en.wikipedia.org/wiki/The_O2_Arena#/media/File:ATP_World_Tour_Final_Tennis_at_The_02_Arena_London.jpg⟩,.

[74] Getty Images/World Para Swimming, The Aquatics Center getting ready to host the Paralympic swimming events in 2012, (n.d.). ⟨https://www.paralympic.orgnewslondon-2012-aquatics-centre-finished⟩.

[75] Architects + Artisans, new-palau-blaugrana_seating-bowl-diagram_courtesy-hok-and-tac. ⟨http://architectsandartisans.combarcelonas-new-arena-by-hok⟩.

[76] Amalgam, Barcelona Sports Arena – 11500 Scale Model, 2016. ⟨https://www.amalgam-models.co.uk/portfolio-item/hok-barcelona-model/⟩,.